

# PCCP

Accepted Manuscript



This is an *Accepted Manuscript*, which has been through the Royal Society of Chemistry peer review process and has been accepted for publication.

*Accepted Manuscripts* are published online shortly after acceptance, before technical editing, formatting and proof reading. Using this free service, authors can make their results available to the community, in citable form, before we publish the edited article. We will replace this *Accepted Manuscript* with the edited and formatted *Advance Article* as soon as it is available.

You can find more information about *Accepted Manuscripts* in the [Information for Authors](#).

Please note that technical editing may introduce minor changes to the text and/or graphics, which may alter content. The journal's standard [Terms & Conditions](#) and the [Ethical guidelines](#) still apply. In no event shall the Royal Society of Chemistry be held responsible for any errors or omissions in this *Accepted Manuscript* or any consequences arising from the use of any information it contains.

# Dynamics of metal uptake by charged soft biointerphases: impacts of depletion, internalisation, adsorption and excretion.

Jérôme F. L. Duval,<sup>1,2</sup>\* Elise Rotureau<sup>1,2</sup>

<sup>1</sup> CNRS, LIEC (Laboratoire Interdisciplinaire des Environnements Continentaux),  
UMR7360, Vandoeuvre-lès-Nancy F-54501, France.

<sup>2</sup> Université de Lorraine, LIEC, UMR7360, Vandoeuvre-lès-Nancy, F-54501, France.

Corresponding author:

\* Jérôme F.L. Duval. E-mail address: jerome.duval@univ-lorraine.fr (J.F.L. Duval)

Tel: + 33 3 83 59 62 63. Fax: + 33 3 83 59 62 55.

## Abstract.

A comprehensive theory is elaborated for the dynamics of metal ion uptake by charged spherical microorganisms. The formalism integrates the interplay over time between bulk metal depletion, metal adsorption, metal excretion (efflux) and transport of metals by conductive diffusion toward the metal-consuming biomembrane. The model further involves the basic physicochemical features of the microbial interphase in terms of size, distribution of electrostatic charges and thickness of peripheral soft surface appendage. A generalization of the Best equation is proposed and leads to the expression of the time-dependent concentration of metal ions at the active membrane surface as a function of bulk metal concentration. Combination of this equation with metal conservation condition over the sample volume allows a full evaluation of bulk metal depletion kinetics and the accompanying time-dependent uptake and excretion fluxes as a function of metal-microorganism electrostatic interaction, microbe concentration and relevant biophysicochemical features of the interphase. Practically tractable expressions are derived in the limit where the Biotic Ligand Model (BLM) is obeyed and in situations where conductive diffusion transport of metals significantly determines the rate of biouptake. In particular, the plateau value reached at sufficiently long times by bulk metal concentration is rigorously expressed in terms of the key parameters pertaining to the adsorption process and to the kinetics of metal uptake and excretion. The theory extends and unifies previous approximate models where the impacts of extracellular metal transport and/or metal efflux on the overall rate of uptake were ignored.

*Keywords:* Biouptake, Depletion, Adsorption, Excretion, Electrostatics, Transport, BLM.

## 1. Introduction.

The uptake of metal ions by microorganisms is mediated by interfacial processes encompassing metal transport in the medium, adsorption at the microorganism surface, internalisation and excretion following transfer through the membrane.<sup>1,2</sup> The interplay between the kinetics of metal internalisation and the rate of diffusive metal supply from bulk solution to the biosurface defines a general dynamic situation in which metal transfer kinetics across the membrane barrier and metal transport in the extracellular volume play key roles.<sup>3,4</sup> For metal-complexing media involving particulate and/or molecular ligands, the situation becomes more complex in that bioavailability of metals to microorganisms may be impacted by the dynamics of metal speciation in solution, *i.e.* the kinetics of interconversion between the relevant metal species.<sup>4,5</sup> The widely used and simplified Biotic Ligand Model (BLM) for metal biouptake and toxicity, is based on the prerequisite that the rate of metal supply is infinitely fast compared to actual uptake.<sup>4-6</sup> Therefore, BLM exclusively applies to cases where metal species in the bulk solution are in constant equilibrium with the sensitive internalisation sites on the biological surface. While numerous data collected for microorganisms or algae were satisfactorily interpreted by BLM, several documented examples of its failure may also be found under complexing and non-complexing conditions.<sup>1-12</sup> This simply reflects that this equilibrium approach approximates a limiting case of the more involved dynamic situation, where both the rate of metal supply and the kinetics of transfer across the biointerface may be operational. Despite their respective merits, current dynamic and equilibrium modelling still fails in offering a *generic* theoretical basis for data interpretation, which is essentially due to two reasons:

First, available models do not explicitly integrate the charged interphasial region separating the biomembrane and the outer electrolyte solution. This interphase is however generally the location of charged 3D polymeric compounds such as exopolysaccharides, lipopolysaccharides, fimbriae or other surface appendages that may protrude several tens to hundreds of nanometers from the supporting active membrane.<sup>13-18</sup> This soft (*e.g.* porous) biointerphase<sup>17</sup> significantly mediates electrostatic and steric interactions with compounds such as metals, cytotoxic polymer materials or nanoparticles.<sup>19-21</sup> Recent experimental reports further highlight the role played by these extracellular structures in trapping toxic chemicals *via* adsorption or in screening strongly-binding functional groups of the cell wall, thereby modifying the partitioning of the contaminants across the biointerphase.<sup>21-24</sup> Additionally, conductive diffusion transport of metallic contaminants from solution to active membrane may be significantly retarded when crossing such surface structures, which represents a protection mechanism against toxic effects over time.<sup>25,26</sup> As a remark, soft surface structures confer peculiar electrokinetic properties upon microbes that are now well supported at both experimental and theoretical levels.<sup>17,18,27,28</sup>

Secondly, current models for metal biouptake never integrate the entire range of interfacial processes that likely occur at complex biointerphases. Some account for the dynamic interplay between metal

diffusion supply and internalisation under steady-state conditions<sup>5,29</sup> following the pioneering strategy by Best,<sup>30</sup> and omit the respective contributions of excretion (efflux) and adsorption in the balance between intracellular and extracellular metal concentrations. Others integrate internalisation and excretion, *albeit* with assuming *a priori* that metal surface concentration identifies with bulk metal concentration.<sup>31</sup> This approximation is in line with the restrictive equilibrium BLM applied to the situation of uncharged microorganisms, a case that is never met in practice,<sup>29</sup> or to situations where background electrolyte concentration is sufficiently large to screen all charges carried by the biointerphase.<sup>29</sup> The latter condition is however rarely applicable for freshwater whose typical salinity is of the order of 1 mM. The (apparent) rates of metal biouptake reported in current literature do not generally represent the true rate constant of membrane transfer of target species because the pH- and ionic strength-dependent electrostatic properties of the microorganisms are commonly ignored. Such approximation is inappropriate at sufficiently low salinity and/or large microbial charges, even more so since electrostatics modify both the metal partitioning across the biomembrane and the kinetics of the various biointerfacial processes like internalisation.<sup>29</sup> Numerous studies further investigate metal ‘bioaccumulation’ at microbial interfaces on the sole basis of classical equilibrium and/or kinetic adsorption data fitted to *ad hoc* Langmuir and Freundlich expressions, or to empirical pseudo-second-order kinetic models.<sup>32-34</sup> Finally, the accounts of bulk metal depletion effects on biouptake kinetics are scarce, apart from few exceptions.<sup>29,31,35</sup> Such effects are however critical for practical systems like biofilms or bioreactors,<sup>35</sup> and their measurement are extremely valuable for retrieving basic uptake parameters.<sup>29,31,35</sup>

In view of the diversity for processes that potentially control synergistically or competitively metal uptake at complex biointerphases, it is timely to develop a theory where the key physicochemical aspects of soft microbial interphases are implemented together with the *joint* impacts of extracellular metal transport, metal depletion in solution, adsorption, excretion and internalisation. Such modelling is mandatory for analysing data collected under a wide range of conditions (including medium pH, salinity and cell concentration) for microbes with different surface structures and distinct abilities to deal with metals over time. The main objective of this work is to develop such a formalism. While the coupling between the equations governing metal transport, internalisation-excretion kinetics and adsorption requires numerical solutions that are provided here, it is demonstrated that some practical situations may be solved analytically with tractable expressions for the relevant measurable metal fluxes and bulk metal concentration. These cases correspond to the extremes in the spectrum of metal bioaffinity for internalisation sites on the biomembrane. It is further shown that previous models on metal biouptake in non-complexing media<sup>29,31,35</sup> correspond to limits of the theory detailed here. In particular, a generalisation of the Best equation,<sup>30</sup> used to interconnect surface and bulk metal concentrations with full account of metal transport, internalisation and

excretion fluxes, is derived. Combining this equation with metal conservation condition across sample volume allows for quantifying the adsorbed, excreted, depleted and internalised metal fractions over time.

## 2. Description of the problem.

Consider a spherical microorganism (*e.g.* a bacterium) of radius  $a$  with a charged membrane surrounded by a charged soft surface layer of thickness  $d$ , as specified in Figure 1 where the radial coordinate  $r$  is defined. The nomenclature is identical to that of our recent work<sup>29</sup> where metal excretion and adsorption processes were ignored. The microbial soft surface layer may extend a few nms to several hundred nms from the membrane, its origin may be biotic or it may result from the adsorption of charged organic or inorganic materials.<sup>29</sup> A Kuwabara cell representation is adopted where an individual microorganism is surrounded by a virtual cell of radius  $r_c$  such that the bioparticle/solution volume ratio in the unit cell equals the bioparticle volume fraction over the entire system, *i.e.*  $r_c = r_0 \varphi^{-1/3}$  where  $r_0 = a + d$  and  $\varphi = r_0^3 c_P$  is the volume fraction of microorganisms with  $c_P$  the microorganism number concentration. Let  $M^{z_M}$  be a metal ion  $M$  of valence  $z_M$  present in the medium and the bulk concentration of  $M^{z_M}$ , denoted as  $c_M^*(t)$ , identifies with the local concentration  $c_M(r, t)$  in  $M^{z_M}$  taken at the position  $r = r_c$ .  $c_M^*$  depends on time  $t$  because the possibility of metal depletion by the microorganisms is accounted for in this work. In agreement with practical cases, the medium further contains an indifferent  $z : z$  background electrolyte of bulk concentration  $c^\infty$  in excess compared to the metal traces,<sup>29,31,35</sup> *i.e.*  $c^\infty / c_M^*(0) \gg 1$ . It is recognized that biointerphases are generally defined by a diffuse (gradual) profile for the density of soft material surrounding the membrane.<sup>17,29</sup> This is accompanied by a modification of the electrostatic potential distribution compared to the situation where a step-function profile is adopted, which in turn may affect the conduction contribution to metal transport across the biointerphase.<sup>17</sup> A gradual distribution of soft surface material density further possibly leads to a position-dependent metal diffusion coefficient and dielectric permittivity, the former resulting from increased steric interaction between microbe and metals crossing the diffuse soft surface layer, and the latter from a radial distribution of the hydrophobic/hydrophilic balance across the layer up to the membrane.<sup>29,36,37</sup> Integrating these aspects inherently connected to the nature of the peripheral material density profile, makes it impossible the analytical derivation of target metal species partitioning across the membrane and the capture of the respective contributions of transport, internalisation and excretion to the overall dynamics of metal biouptake.<sup>29</sup> Since the purpose of this work is to clearly define these contributions and to provide experimentalists practical ‘tools’ for data interpretation, we have chosen here the simplest route offered by the step-function representation. The account of biointerfacial diffuseness is possible with the results given in the first paper of this series on metal uptake dynamics<sup>29</sup> (see

Supporting Information therein) where modifications of the governing metal transport and electrostatic equations are detailed for a diffuse radial profile of the soft surface material density. Within the framework of the here adopted step-function profile across the biointerphase, metals diffuse toward the microorganism and the diffusion coefficients of  $M^{z_M}$  within and outside the soft surface layer are denoted as  $D_{M,in}$  and  $D_{M,out}$ , respectively, with  $\varepsilon = D_{M,in}/D_{M,out} \leq 1$ .<sup>29</sup> In addition, we introduce  $\hat{A} = \varepsilon_s/\varepsilon_r$  the ratio between relative dielectric permittivities in the soft surface layer and in the outer solution. In this work, the number of cells is fixed, and their multiplication and death are therefore not accounted for. This tacitly implies that the developments reported here are valid pending the use of minimum essential media where the density of alive cells remains constant over time.<sup>31</sup> The most complex situations where microbial growth kinetics and toxicokinetics are coupled to metal biouptake dynamics will be the subject of a separate study.

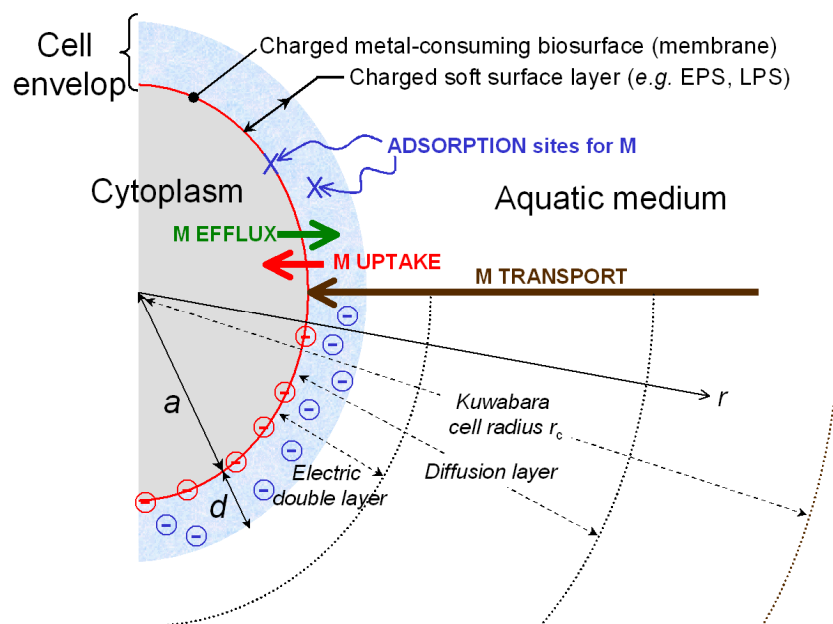


**Figure 1.** Scheme of the processes governing metal biouptake at charged soft biointerphases.

The equations governing biouptake, adsorption, excretion and metal transport are detailed in the following paragraphs.

**Biouptake.** The metal uptake flux at time  $t$ ,  $J_u(t)$ , is defined by a Michaelis-Menten mechanism which corresponds to the fast Langmuirian adsorption of  $M^{z_M}$  at the internalisation sites compared to metal transport, followed by a first order rate-limiting internalisation step<sup>29,35</sup>

$$J_u(t)/J_u^* = c_M^a(t)/[K_M + c_M^a(t)], \quad (1)$$

where  $c_M^a(t)$  is the time-dependent metal concentration at the membrane surface,  $K_M$  is the characteristic (intrinsic) affinity of  $M^{z_M}$  for the internalisation sites,  $J_u^* = k_{\text{int}} K_H K_M$ <sup>29</sup> is the limiting (maximum) uptake flux reached for  $K_M \ll c_M^a(t)$  with  $k_{\text{int}}$  and  $K_H$  the intrinsic kinetic constant for internalisation and the true metal adsorption coefficient in the linear portion of the Langmuir isotherm (Henry regime), respectively. The metal surface concentration involved in eqn (1) must be corrected for electrostatics,<sup>29</sup> which requires solving metal transport equation with account of conduction contribution, as detailed below in the section entitled ‘Transport’. For the sake of simplicity, the existence of a single type of internalisation site at the membrane surface is assumed, which is surely restrictive with respect to real biological cells. Without loss of generality, the developments detailed in §3, 4 and 5 may be extended to cases where  $N$  different internalisation sites are considered. The total flux of metals taken up can then be decomposed into the sum of  $N$  Michaelis-Menten uptake fluxes with the corresponding limiting flux  $J_{u,j=1,\dots,N}^*$  and metal affinity  $K_{M,j=1,\dots,N}$ .

**Adsorption.** Prior to uptake, metal ions adsorb on the internalisation sites. They may adsorb as well on mere adsorption sites that do not lead to internalisation and that are distributed over the 2D charged membrane surface and/or the 3D charged soft surface structure at the periphery of the microorganism (Figure 1). Adsorption processes are generally faster than transport, internalisation and excretion, so equilibrium relationships may be applied to relate *local* concentrations of adsorbed and free metals.<sup>2,31</sup> In this study, we therefore ignore the very adsorption/desorption dynamics of metals to/from non-transporter ligands across the surface layer and at the membrane surface. This approximation conforms to that done by previous authors who exclusively considered non-transporter sites at the membrane surface.<sup>31,35</sup> It may however be severe for metals like Fe(III) whose complex formation with any ligand is expected to be strongly rate-limited by the slow removal of water from inner coordination sphere (Eigen mechanism). The current model thus applies to all cases where the characteristic rates of internalisation and transport are much lower than the typical dehydration and desorption rates of metal ions. For other cases where metal adsorption/desorption to/from the ligands in the soft surface layer and at the membrane surface proceeds with dynamics comparable to that of transport and/or internalisation processes, it becomes mandatory to amend eqns (2)-(3) and explicitly include the relevant metal adsorption/desorption time scales. For the sake of simplicity and without loss of generality, we shall consider in this work metal adsorption on two types of sites, one located at the membrane surface and another distributed across the soft surface layer. Accordingly, the time-dependent surface concentration  $\Gamma^S(t)$  of adsorbed metals at the membrane surface is provided by

$$\Gamma^S(t)/\Gamma_{\max}^S = c_M^a(t)/\left[K_M^S + c_M^a(t)\right], \quad (2)$$

where  $\Gamma_{\max}^S$  is the total surface concentration of adsorption sites on the membrane,  $K_M^S$  is the affinity coefficient of  $M^{z_M}$  and the quantity  $K_H^S = \Gamma_{\max}^S / K_M^S$  corresponds to the Henry adsorption coefficient. The situation where metal adsorption on the internalisation sites is most significant corresponds to  $K_M^S = K_M$  (or  $K_H^S = K_H$ ). The time-dependent amount  $Q^V(t)$  of adsorbed metals across the soft surface structure is expressed by the integral equation

$$Q^V(t) = 4\pi\rho_{\max}^V \int_a^{r_0} \left\{ c_M(r,t) / \left[ K_M^V + c_M(r,t) \right] \right\} r^2 dr, \quad (3)$$

with  $\rho_{\max}^V$  the volume density of adsorption sites carried by the soft surface layer and  $K_M^V$  the corresponding metal affinity parameter. As for eqn (1), eqns (2) and (3) may be adapted to cases that require the introduction of several types of adsorption sites on the membrane and through the soft surface layer. Within the linear Henry adsorption regime, these cases can be formulated using a single Henry isotherm with Henry coefficient that is a weighted average of the Henry coefficients pertaining to the various internalisation sites and mere adsorption sites considered.<sup>2</sup>

**Excretion.** The excretion flux, or efflux  $J_e(t)$ , reflects the possibility that an organism elaborates strategies over time to expel potentially toxic chemicals from their intracellular volume. As a first approach, the efflux rate is set proportional to the amount  $\phi_u(t)$  of metals internalised at time  $t$  by the microorganism,<sup>31</sup> so that

$$J_e(t) = k_e \phi_u(t), \quad (4)$$

where  $k_e$  is the kinetic constant for excretion and  $\phi_u$  is the concentration of internalized metals per microorganism surface area.

**Transport.** As detailed in a previous report,<sup>29</sup> the reestablishment of the here-considered steady-state metal concentration profile at any time  $t$  following depletion is considered as instantaneous, which is valid provided that the inequality  $r_0 \ll r_c$  is verified,<sup>29,35</sup> a condition that is in line with practical values of  $\varphi$ . The above approximation deserves further comments. For metals with charge numbers higher than that of ions from background electrolyte, the characteristic equilibration time of  $M^{z_M}$  in the interphasial electric double layer is larger than that of the background electrolyte ions by a factor that is proportional to a Boltzmann accumulation term, as detailed by van Leeuwen and collaborators in their analysis of relaxation processes involved in chemodynamics of metal-(nano)particulate ligands.<sup>38,39</sup> Within the framework of the

current study, developments are therefore valid for characteristic depletion (and internalisation) time scales that are much larger than the time constant for distribution of  $M^{z_M}$  to achieve re-equilibration. Within these limits, the expressions at time  $t$  for the metal concentrations within and outside the charged soft surface layer read as<sup>29</sup>

$$c_M(a \leq r \leq r_o, t) = b_r c_M^*(t) \frac{c_M^a(t) b_a^{-1} / c_M^*(t)}{1 + l^{-1} F_{a,r}} l^{-1} F_{a,r} \quad (5)$$

and

$$c_M(r_o \leq r \leq r_c, t) = b_r c_M^*(t) \frac{c_M^a(t) b_a^{-1} / c_M^*(t) - 1}{1 + F_{a,r_o} l^{-1}} \frac{F_{r,r_c}}{F_{r_o,r_c}} \quad (6)$$

respectively. The quantity  $b_r = \exp(-z_M y(r)/z)$  stands for the Boltzmann factor at the position  $r$  with  $y(r) = zFy(r)/RT$  the dimensionless electrostatic potential at that position,  $F$  the Faraday number,  $T$  the temperature,  $R$  the gas constant and  $y(r)$  the potential.  $b_a$  corresponds to the Boltzmann factor  $b_{r=a}$  evaluated at the membrane surface and  $y(r)$  defines the equilibrium electrostatic interaction taking place between the charged microorganism of Figure 1 and the metal ions carrying the charge  $z_M e$ .  $y(r)$  is independent of  $t$  because (i) the excess in background electrolyte ions over  $M^{z_M}$  maintains equilibrated electric double layers whose relaxation (typically in the  $\mu s$  range) is extremely fast compared to internalisation and because we tackle cases where equilibration time of  $M$  in the interfacial electric double layer is fast as compared to the time scales of the other relevant interfacial processes, and (ii) the amount of charges carried by the biointerphase is constant over time as it is supposedly large compared to the quantity of adsorbed trace metals. The evaluation of potential distribution  $y(r)$  is based on numerically solving the non-linear Poisson-Boltzmann equation, as detailed elsewhere.<sup>29</sup> The sign and magnitude of  $y(r)$  are intimately related to the structure of the biointerphase, which includes the thickness, the hydrophobic/hydrophilic balance and the volume charge density of the microbial soft surface layer, as well as the microorganism size and the membrane surface charge density (Figure 1). For further details on the evaluation of  $y(r)$ , the reader is referred to Ref. [29] where analytical expressions are provided under conditions where (i) the biointerphase is poorly to moderately charged, (ii) the overall charge carried by the microorganism is significantly screened by ions from background electrolyte, and (iii) the thickness of the peripheral soft surface layer is large compared to the extension of the Debye layer (Donnan situation). The

function  $F_{r_1, r_2}$  involved in eqs (5)-(6) is defined by the integral  $F_{r_1, r_2} = \int_{r_1}^{r_2} r^{-2} b_r^{-1} dr$  where  $r_1$  and  $r_2$  are

dummy variables, and the scalar  $\lambda$  is given by  $\lambda = -(\varepsilon F_{r_o, r_c} + F_{a, r_o}) = -\varepsilon a^{-1} / f_{el}$ , with  $f_{el}$  the factor that

corrects the diffusion flux for the acceleration or retardation of  $M^{z_M}$  due to the electric double layer field<sup>29,40</sup>

$$f_{el} = (ef_{el,in} - f_{el,out}) / (ear_0^{-1} f_{el,in} + f_{el,out}). \quad (7)$$

$f_{el,in} = 1/(aF_{a,r_0})$  and  $f_{el,out} = 1/(r_0 F_{r_0,r_c})$  correspond to the electrostatic corrections of the  $M^{z_M}$  diffusion inside and outside the soft surface layer, respectively.<sup>29,40</sup> Using eqn (5), the steady-state conductive diffusion flux  $J_M$  of metals at the membrane surface may be written in the concise form:<sup>29</sup>

$$J_M(t) = J_M^*(t) \left( 1 - c_M^a(t) b_a^{-1} / c_M^*(t) \right), \quad (8)$$

where  $J_M^*(t) = D_{M,out} f_{el} c_M^*(t) / a$  is the limiting conductive diffusion flux reached for  $c_M^a(t) b_a^{-1} / c_M^*(t) \ll 1$ .

Given eqns (1)-(8) that determine the distribution of  $M^{z_M}$  over space and time across the biointerphase, the task is to express the time-dependent bulk and surface metal concentrations as a function of the key biophysicochemical parameters describing internalisation (*i.e.*  $J_u^*$  and  $K_M$ ), excretion ( $k_e$ ), and adsorption ( $\Gamma_{max}^S$ ,  $K_M^S$ ,  $\rho_{max}^V$  and  $K_M^V$ ). Once  $c_M^*(t)$  and  $c_M^a(t)$  are known, all other measurable quantities, including internalisation and excretion fluxes, may be derived from eqns (1)-(4).

### 3. Expressions for the time-dependent surface and bulk metal concentrations.

#### 3.1. Generalization of the Best equation.

Under steady-state conditions, the conductive diffusion flux  $J_M(t)$  of metals from bulk solution to membrane surface equals the sum of the internalisation flux minus the excretion flux

$$J_M(t) = J_u(t) - k_e f_u(t). \quad (9)$$

An important point is that, under steady-state, adsorption processes described by eqns (2) and (3) are not involved in eqn (9), though they contribute to the partitioning of metals across the membrane,<sup>29,35</sup> as further detailed in §4. Variation in the internalized amount of metals with time results from the balance between internalisation and excretion fluxes according to<sup>31</sup>

$$df_u(t)/dt = J_u(t) - J_e(t) = J_u(t) - k_e f_u(t), \quad (10)$$

where the second equality stems from the use of eqn (4). Solving the differential eqn (10) for  $f_u(t)$ , we get:

$$f_u(t) = e^{-k_e t} f_u(0) + \int_0^t J_u(x) e^{k_e x} dx. \quad (11)$$

where  $x$  is a dummy integration variable and  $f_u^0 = f_u(t=0)$ . In the limit  $k_e \rightarrow 0$ , efflux is insignificant

and the classical definition  $f_u(t) = f_u^0 + \int_0^t J_u(x) dx$  for the internalised amount of  $M^{\bar{z}_M}$  is recovered.<sup>41</sup>

This quantity is particularly relevant for addressing metal toxicity. Differentiating eqn (9) with respect to time and using eqn (10) leads to

$$dJ_u(t)/dt - dJ_M(t)/dt = k_e J_M(t). \quad (12)$$

Replacing  $J_u(t)$  and  $J_M(t)$  in eqn (12) by eqn (1) and (8), respectively, we obtain the following relationship between surface and bulk metal concentrations

$$dc_M^*(t)/dt = -k_e c_M^*(t) + K_M b_a^{-1} \left[ k_e \bar{c}_M^a(t) + 1 + Bn^{-1} \left( \frac{d}{dt} + \bar{c}_M^a(t) \right) \frac{d\bar{c}_M^a(t)}{dt} \right], \quad (13)$$

where we have introduced the normalized metal surface concentration  $\bar{c}_M^a(t) = c_M^a(t)/K_M$  as well as the dimensionless ‘bioavailability’ number, denoted  $Bn$ , defined by<sup>29</sup>

$$Bn = (D_{M,out} f_{el} a^{-1}) / (k_{int} K_H b_a). \quad (14)$$

$Bn$  corresponds to the ratio between  $1/(k_{int} K_H b_a) \circ R_s$  and  $1/(D_{M,out} f_{el} a^{-1}) \circ R_T$ , with  $R_s$  denoting the membrane transfer resistance reflecting the ability of  $M$  to cross the membrane surface barrier, and  $R_T$  the resistance of the extracellular compartment to conductive diffusion transport of  $M$ .<sup>29</sup> The general solution of eqn (13) may be written in the transcendental integral form

$$c_M^*(t) = \left( K_M \beta_a^{-1} Bn^{-1} - k_e \phi_u^0 R_T \right) e^{-k_e t} + K_M \beta_a^{-1} \left\{ \bar{c}_M^a(t) - Bn^{-1} \left[ \frac{1}{1 + \bar{c}_M^a(t)} - k_e e^{-k_e t} \int_0^t \frac{e^{-k_e \xi}}{1 + \bar{c}_M^a(\xi)} d\xi \right] \right\}. \quad (15)$$

In the specific cases  $k_e \rightarrow 0$  and/or  $t=0$ , eqn (15) reduces to (Supporting Information)

$$c_M^a / c_M^* = \beta_a \left\{ \left[ 1 - A - B(1 - \omega^0) \right] + \left\{ \left[ A + B(1 - \omega^0) - 1 \right]^2 + 4A(1 + B\omega^0) \right\}^{1/2} \right\} / 2, \quad (16)$$

where the time dependence of  $c_M^a(t)$  and  $c_M^*(t)$  are dropped for the sake of conciseness, and the dimensionless ratio  $\omega^0 = k_e \phi_u^0 / J_u^*$  between efflux at  $t=0$  and limiting uptake flux  $J_u^*$  is introduced. In eqn (16),  $A = K_M / (\beta_a c_M^*)$  and  $B = J_u^* R_T / c_M^*$  refer to the dimensionless (time-dependent) metal-surface bioaffinity parameter and metal bioconversion capacity of the microorganism, respectively.<sup>4,29</sup> Note that  $Bn$  may be written as  $Bn = A/B$ . For  $\omega^0 = 0$ , eqn (16) simplifies into the relationship established by Duval under the condition where there is no efflux at  $t \geq 0$ .<sup>29</sup> In the further extremes where electrostatic

effects are ignored for microorganisms either deprived of a soft surface layer ( $d \rightarrow 0$ ) or whose surface appendages do not hinder metal diffusion ( $\varepsilon \rightarrow 1$ ), eqn (16) identifies with the original equation by Best.<sup>30</sup> Equation (15) may thus be viewed as an original generalization of these previous results as it connects surface and bulk metal concentrations with account of extracellular conductive diffusion transport of M, internalisation *and* excretion by charged soft biointerphases. The full evaluation of  $c_M^*(t)$  and  $c_M^a(t)$  requires an additional equation that stems from the condition of metal conservation within the Kuwabara unit cell.

### 3.2. Derivation of the metal conservation condition.

At any time  $t$ , the extent of depletion of free (*i.e.* non-adsorbed) metal ions in the extracellular volume ( $a \leq r \leq r_c$ ) results from the disappearance of M following internalisation, adsorption on the biomembrane and across the soft surface structure and from pumping M out of the intracellular volume. Within the framework of the Kuwabara representation in Figure 1, this metal balance condition is written

$$4\pi \int_a^{r_c} r^2 [c_M(r,t) - c_M(r,0)] dr = -S_a \left\{ \int_0^t [J_u(\xi) - k_e \phi_u(\xi)] d\xi + \Gamma^S(t) \right\} - Q^V(t), \quad (17)$$

with  $S_a = 4\pi a^2$  the surface area of the nude microorganism (*i.e.* without the peripheral soft surface layer).

Using eqns (10), (11) and (17), and deriving with respect to  $t$  yields

$$\int_a^{r_c} r^2 \left\{ dc_M(r,t)/dt + k_e [c_M(r,t) - c_M(r,0)] \right\} dr = a^2 \left\{ -J_u(t) + k_e \phi_u^0 - [k_e \Gamma^S(t) + d\Gamma^S(t)/dt] \right\} - (4\pi)^{-1} [k_e Q^V(t) + dQ^V(t)/dt], \quad (18)$$

where  $c_M(r,t)$ ,  $J_u(t)$ ,  $\Gamma^S(t)$  and  $Q^V(t)$  depend on  $c_M^*(t)$  and/or  $c_M^a(t)$  according to eqns (5)-(6), (1), (2) and (3), respectively. The differential eqn (18) and the generalized Best eqn (15) (derived from eqn (13)) are coupled and rigorously define the time evolution of the intertwined surface and bulk metal concentrations. In the developments that follow, solutions for  $c_M^a$  and  $c_M^*$  as a function of  $t$  and of the basic biophysicochemical parameters of the problem are given. For the sake of demonstration, this is done first for situations where adsorption may be ignored (§4),<sup>29,35</sup> thus focusing on the impacts of transport-internalisation-excretion processes, then for cases where it is accounted for (§5).

### 4. Situations where metal adsorption may be ignored in eqn (18).

They correspond to a fast initial decrease of the bulk metal concentration as a result of rapid adsorption, delay after which metal transport, internalisation and excretion govern metal partitioning across the

biointerphase over time.<sup>29,35</sup> Under such conditions, the initial bulk metal concentration  $c_M^*(t=0)$  in eqn (16) identifies with the concentration of metals introduced in the sample volume and corrected for the adsorbed amount at the biointerphase. Then, eqn (18) may be simplified with specifying  $\Gamma^S(t)=0$ ,  $Q^V(t)=0$  and upon further substitution therein of eqns (5)-(6) and (1) for the metal concentration profile  $c_M(r,t)$  and the uptake flux  $J_u(t)$ , respectively. After subsequent elimination of  $c_M^*(t)$  by means of eqn (13) and lengthy developments detailed in Supporting Information, one obtains the elegant differential equation for  $\bar{c}_M^a(t)$

$$\left\{ \frac{(\tau_L - \tau_E) - \tau_L [1 + \bar{c}_M^a(t)^2]}{[1 + \bar{c}_M^a(t)] [\bar{c}_M^a(t) - \bar{c}_+] [\bar{c}_M^a(t) - \bar{c}_-]} \right\} d\bar{c}_M^a(t) = k_e \tau_L dt, \quad (19)$$

where  $\tau_L$  and  $\tau_E$  are the characteristic timescales recently derived for the kinetics of bulk metal depletion in the absence of excretion.<sup>29</sup> In this limit where  $k_e \rightarrow 0$ ,  $\tau_L$  refers to cases where the rate of M depletion is limited solely by the internalisation process and  $\tau_E$  pertains to situations where the depletion rate may be determined both by the internalisation and conductive diffusion transport of M. The expressions of  $\tau_L$  and  $\tau_E$  read as<sup>29</sup>

$$\tau_L = 4\pi R_S G_{a,r_c} / S_a, \quad (20)$$

and

$$\tau_E = \tau_L - J_u^* \Omega_1 R_T, \quad (21)$$

with

$$\Omega_1 = - \left[ G_{r_o, r_c} - \left( 1 - \varepsilon^{-1} f_{el} / f_{el, in} \right) H_{r_o, r_c}^{r_c} / F_{r_o, r_c} - H_{a, r_o}^a a \varepsilon^{-1} f_{el} \right] / \left( a^2 J_u^* \right), \quad (22)$$

with  $\Omega_1 \leq 0$  (Supporting Information),  $G_{r_1, r_2} = \int_{r_1}^{r_2} r^2 \beta_r dr$  and  $H_{r_1, r_2}^{r_3} = \int_{r_1}^{r_2} r^2 \beta_r F_{r, r_3} dr$ . As extensively discussed elsewhere,<sup>29</sup>  $\tau_L$  and  $\tau_E$  depend on the microorganism volume fraction  $\varphi$  (subsumed in the Kuwabara cell radius  $r_c$ ) and integrate the basic physicochemical descriptors of the biointerphase depicted in Figure 1, since they involve the potential distribution  $y(r)$  as well as the ability of M to diffuse through the soft surface layer. For further details, the reader is referred to Ref. [29] where expressions of  $\tau_L$  and  $\tau_E$  are detailed for biointerphases whose electrostatic features obey the Donnan condition. The constants  $\bar{c}_\pm$  in eqn (19) are defined by (Supporting Information)

$$\bar{c}_\pm = (2k_e \tau_L)^{-1} \left\{ - [1 + k_e (\tau_L + \tau_o)] \pm [1 + 2k_e (\tau_L + \tau_o) + k_e^2 (\tau_L - \tau_o)^2]^{1/2} \right\}, \quad (23)$$

with  $\bar{c}_+ \geq 0$ ,  $\bar{c}_- \leq 0$  and  $-\tau_o > 0$  is a time constant that depends on the initial concentrations of M at the membrane surface and in the bulk solution, as well as on the initial amount of internalized metals

$$\tau_o = \Omega_1 c_M^*(0) + 2\Omega_2 \beta_a^{-1} c_M^a(0) - \phi_u^0 / J_u^*, \quad (24)$$

with  $\Omega_2 = -\left[\Omega_1 + G_{a,r_c} / (a^2 J_u^*)\right] / 2 \leq 0$ . As shown in Supporting information,  $-\tau_o$  satisfies

$$J_u^* \times (-\tau_o) = 4\pi \int_a^{r_c} r^2 c_M(r, t) dr / S_a + \phi_u^0 \text{ and thus physically corresponds to the time required for the}$$

microorganism to internalize the total amount of metal ions in solution at  $t = 0$ ,  $4\pi \int_a^{r_c} r^2 c_M(r, 0) dr / S_a + \phi_u^0$ ,

under conditions where the uptake flux is  $J_u^*$ . The value of  $c_M^a(0)$  in eqn (24) is derived from the initial bulk metal concentration  $c_M^*(0)$  using eqn (16). The exact solution to eqn (19) may be written in the transcendental form

$$\ln \left\{ \frac{\left[ \frac{\bar{c}_M^a(t) - \bar{c}_-}{\bar{c}_M^a(0) - \bar{c}_-} \right]^{p_-(1+\bar{c}_+)}}{\left[ \frac{\bar{c}_M^a(t) - \bar{c}_+}{\bar{c}_M^a(0) - \bar{c}_+} \right]^{p_+(1+\bar{c}_-)} \left[ \frac{1 + \bar{c}_M^a(t)}{1 + \bar{c}_M^a(0)} \right]^{(\tau_E - \tau_L)(\bar{c}_+ - \bar{c}_-)}} \right\} = k_e \tau_L (1 + \bar{c}_+) (1 + \bar{c}_-) (\bar{c}_+ - \bar{c}_-) t, \quad (25)$$

with  $p_{\pm} = \tau_L \bar{c}_{\pm}^2 + 2\tau_L \bar{c}_{\pm} + \tau_E$ . Once  $c_M^a(t)$  is known from eqn (25),  $c_M^*(t)$  can be estimated according to eqn (15).

Inspection of eqns (19) and (25) reveals that the limit  $t \rightarrow \infty$  corresponds to  $\bar{c}_M^a \rightarrow \bar{c}_+$  and  $d\bar{c}_M^a/dt \rightarrow 0$ . This implies that  $\bar{c}_+$  actually identifies with the value reached by the surface metal concentration  $\bar{c}_M^a$  at sufficiently long times  $t$ , expressed as  $\bar{c}_+ \equiv \bar{c}_M^a(\infty)$ . At  $t \rightarrow \infty$ ,  $d\bar{c}_M^a/dt \rightarrow 0$  necessarily implies  $dJ_u(t)/dt \rightarrow 0$  (obtained from eqn (1)) and combination with eqn (12) then leads to  $c_M^*(\infty) = \beta_a^{-1} c_M^a(\infty)$ , *i.e.* the equilibrium Boltzmann law that guarantees the validity of BLM holds at  $t \rightarrow \infty$ . In the case where excretion is insignificant, we have  $k_e \rightarrow 0$ , and the Taylor expansion of eqn (23) with respect to  $k_e$  leads to  $\bar{c}_M^a(\infty) \rightarrow 0$ , which implies  $c_M^*(\infty) \rightarrow 0$ . This is in agreement with the predictions given in Ref. [29]. For all other cases where  $k_e \neq 0$ ,  $c_M^*(\infty)$  converges on the non-zero plateau value  $\beta_a^{-1} c_M^a(\infty)$  where  $\bar{c}_M^a(\infty)$  is expressed by  $\bar{c}_+$  in eqn (23). This important result basically indicates that examination of depletion kinetic experiments at sufficiently long times makes it possible to identify the

existence of intracellular metal excretion. This is confirmed by the experiments of Hadju et al.<sup>31</sup> who measured a plateau value for  $c_M^*(t \rightarrow \infty)$  in the case of Cd(II) uptake by metal-resistant bacterium *Cupriavidus metallidurans* that elaborates efflux strategies to limit the potential impact of toxic metals on its metabolism. Unlike previous studies,<sup>29,31,35</sup> eqns (15) and (25) (Table 1, case [A]) rigorously define  $c_M^*(t)$  and/or  $c_M^a(t)$  with account of efflux and without *a priori* approximation on how the rate of uptake is limited by conductive diffusion transport of M. In addition, they apply to cases where adsorption-internalisation of M (eqn (1)) does not necessarily fall within the linear Henry regime that is generally adopted to circumvent the non-linear dependence of  $J_u$  on  $c_M^a$ .<sup>31,35</sup>

For a given  $c_M^*(t=0)$ ,  $c_M^*(t)$  and  $c_M^a(t)$  can be computed numerically from eqns (15) and (25) by means of the collocation procedure COLSYS<sup>42</sup> with eqn (16) defining the initial surface concentration  $c_M^a(t=0)$ . The internalisation and excretion parameters involved in  $c_M^*(t)$  and  $c_M^a(t)$  are  $J_u^*$ ,  $K_M$  (or  $J_u^*$  and  $K_H \times k_{\text{int}}$ ) and  $k_e$ . Explicit expressions of  $c_M^*(t)$  and  $c_M^a(t)$  may be further derived in the practical limits  $K_M \ll c_M^a(t)$  and  $K_M \gg c_M^a(t)$  (detailed below).

## Expressions for $c_M^*(t)$ and $\bar{c}_M^a(t) = c_M^a(t)/K_M$

$$\forall K_M: \quad \boxed{\text{A}} \quad \left\{ \begin{array}{l} \ln \left\{ \frac{[\bar{c}_M^a(t) - \bar{c}_-]^{p_-(1+\bar{c}_+)}}{[\bar{c}_M^a(t) - \bar{c}_+]^{p_+(1+\bar{c}_-)} [1 - \bar{c}_M^a(t)]^{(\tau_E - \tau_L)(\bar{c}_+ - \bar{c}_-)}} \right\} = k_e \tau_L (1 + \bar{c}_+) (1 + \bar{c}_-) (\bar{c}_+ - \bar{c}_-) t \\ c_M^*(t) = \left( \frac{K_M}{\beta_a Bn} - k_e \phi_u^0 R_T \right) e^{-k_e t} + \frac{K_M}{\beta_a} \left\{ \bar{c}_M^a(t) - \frac{1}{Bn} \left[ \frac{1}{1 + \bar{c}_M^a(t)} - k_e e^{-k_e t} \int_0^t \frac{e^{-k_e \xi}}{1 + \bar{c}_M^a(\xi)} d\xi \right] \right\} \end{array} \right.$$

$$K_M \ll c_M^a(t): \quad \boxed{\text{B}} \quad \left\{ \begin{array}{l} \bar{c}_M^a(t) = \left( \frac{\beta_a c_M^*(0)}{K_M} + \frac{1 + k_e \tau_o}{k_e \tau_L} \right) e^{-k_e t} - \frac{1 + k_e \tau_o}{k_e \tau_L} \\ c_M^*(t) = \left( c_M^*(0) + \frac{K_M}{\beta_a} \frac{1 + k_e \tau_o}{k_e \tau_L} \right) e^{-k_e t} - \frac{K_M}{\beta_a} \frac{1 + k_e \tau_o}{k_e \tau_L} \end{array} \right.$$

$$K_M \gg c_M^a(t): \quad \boxed{\text{C}} \quad \left\{ \begin{array}{l} \bar{c}_M^a(t) = \left( \bar{c}_M^a(0) + \frac{k_e \tau_o}{1 + k_e \tau_L} \right) e^{-t/\tau_d} - \frac{k_e \tau_o}{1 + k_e \tau_L} \\ c_M^*(t) = \alpha_1 e^{-k_e t} + \frac{K_M}{\beta_a} e^{-t/\tau_d} \left( \bar{c}_M^a(0) + \frac{k_e \tau_o}{1 + k_e \tau_L} \right) \left[ 1 + \frac{Bn^{-1}(1 + k_e \tau_L)}{1 + k_e(\tau_L - \tau_E)} \right] - \frac{K_M}{\beta_a} \frac{k_e \tau_o}{1 + k_e \tau_L} \end{array} \right.$$

$$\text{with } \alpha_1 = -k_e \phi_u^0 R_T - \frac{K_M}{\beta_a Bn} \frac{k_e [\tau_o + \bar{c}_M^a(0) \tau_E]}{[1 + k_e(\tau_L - \tau_E)]}, \quad \tau_d = \frac{\tau_E}{1 + k_e \tau_L} \quad \text{and} \quad c_M^a(0) = \beta_a \left[ \frac{c_M^*(0) + k_e \phi_u^0 R_T}{1 + Bn^{-1}} \right]$$

**Table 1.** Summary of the expressions defining  $c_M^*(t)$  and  $c_M^a(t)$ . Details in the text.

### 4.1. Limit $K_M \ll c_M^a(t)$ (case **B** in Table 1).

This case corresponds to a strong affinity of M for internalisation sites, which simplifies eqn (1) into  $J_u(t) \approx J_u^*$ . After some developments, substitution into eqn (12) and combination with eqn (18) yields expressions of  $c_M^a(t)$  and  $c_M^*(t)$  given in Table 1 (case **B**). It is verified that the only internalisation and excretion parameters involved in  $c_M^a(t)$  and  $c_M^*(t)$  are  $J_u^*$  and  $k_e$ , recalling that the ratio  $K_M/\tau_L$  is independent of  $K_M$ . The reader is referred to the Supporting Information for relevant mathematical details. The equilibrium Boltzmann relationship now systematically holds between surface and bulk metal concentrations, *i.e.* the equation  $c_M^*(t) = \beta_a^{-1} c_M^a(t)$  applies at  $t \geq 0$ . This simplifies eqn (24) for  $\tau_o$  into

$$\tau_o = - \left[ \tau_L \beta_a c_M^*(0) / K_M + \phi_u^0 / J_u^* \right]. \quad (26)$$

The condition  $K_M \ll c_M^a(t)$  thus implies a fast transport of M from solution to biomembrane so that the rate of uptake is only limited by the internalisation process, confirmed by the absence of the time constant  $\tau_E$  (and of the metal transport resistance  $R_T$ , see eqn (21)) in expressions  $c_M^a(t)$  and  $c_M^*(t)$ . The specific case  $K_M \ll c_M^a(t)$  conforms to the equilibrium hypothesis postulated within the framework of the BLM. The characteristic timescale associated with exponential decay of  $c_M^*$  with time  $t$  (Table 1) then simply identifies with  $1/k_e$  provided the condition  $k_e \neq 0$  is respected. In the extreme where efflux is insignificant ( $k_e \rightarrow 0$ ), the Taylor expansion of  $c_M^*(t)$  with respect to  $k_e$  leads to

$$c_M^*(t)/c_M^*(0) \approx 1 - K_M t / (\beta_a c_M^*(0) \tau_L). \quad (27)$$

This linear decrease of  $c_M^*(t)$  with  $t$  correctly reproduces the result derived by Duval<sup>29</sup> in the absence of excretion under the condition  $J_u(t) \approx J_u^*$ . Further examination of the expressions reported in Table 1, case [B], reveals that general expression (23) for  $c_M^*(t \rightarrow \infty) = \beta_a^{-1} c_M^a(t \rightarrow \infty)$  now simplifies into

$$c_M^*(t \rightarrow \infty) \rightarrow -K_M(1 + k_e \tau_o) / (\beta_a k_e \tau_L), \quad (28)$$

where  $-\tau_o$  is positive. For situations where  $k_e \tau_o \ll 1$  (met, in particular, for  $k_e \rightarrow 0$ ), eqn (28) leads to negative values for  $c_M^*(t \rightarrow \infty)$ , and thus a negative  $c_M^a(t \rightarrow \infty)$ . The condition  $K_M \ll c_M^a(t \rightarrow \infty)$  underlying the strict applicability of the developments in §4.1, is then necessarily violated at  $t \rightarrow \infty$  for  $k_e \tau_o \ll 1$ . This marks a restriction in the use of the equations corresponding to case [B] in Table 1.

#### 4.2. Limit $K_M \gg c_M^a(t)$ (case [C] in Table 1).

This inequality corresponds to  $\bar{c}_M^a(t) \ll 1$  and is relevant to cases where adsorption is so weak that the linear Henry regime applies at any  $t$ , *i.e.* eqn (1) becomes  $J_u(t) \approx K_H k_{\text{int}} c_M^a(t)$ . Simplifying eqns (13) and (16) for  $\bar{c}_M^a(t) \ll 1$  and combining with eqn (18) yields the expressions of  $c_M^a(t)$  and  $c_M^*(t)$  reported in Table 1, case [C] (details are given in Supporting Information). In particular,  $\tau_o$  simplifies into  $\tau_o = -\bar{c}_M^a(0) \tau_E - \phi_u^0 (1/J_u^* + k_e \Omega_1 R_T)$  with  $c_M^a(0) = \beta_a [c_M^*(0) + k_e \phi_u^0 R_T] (1 + Bn^{-1})^{-1}$  (Supporting Information). It may be further realized that the only internalisation and excretion parameters involved in  $c_M^a(t)$  and  $c_M^*(t)$  are now  $K_H \times k_{\text{int}}$  and  $k_e$ . For situations where the microorganism does not excrete metals at  $t = 0$ ,  $\phi_u^0 = 0$  and the constant  $\alpha_1$  involved in the expression of  $c_M^*(t)$  becomes zero (Supporting

Information). The only characteristic timescale governing bulk metal depletion kinetics is then defined by  $\tau_d = \tau_E / (1 + k_e \tau_L)$ . For cases where  $\phi_u^0 \neq 0$ , the decrease of  $c_M^*$  with  $t$  is generally determined by the sum of two exponentials with timescales  $\tau_d$  and  $1/k_e$ . Both the prefactor of the exponential decay functions involved in  $c_M^*(t)$  and the depletion timescale  $\tau_d$  involve  $\tau_E$  and thus the transport resistance  $R_T$  (eqn (21)), indicating the rate of metal depletion may be now significantly limited by conductive diffusion supply of M from the solution. This is further reflected by the general inapplicability of the Boltzmann relationship  $c_M^a(t) = \beta_a c_M^*(t)$  at  $t \geq 0$ . As anticipated from the analysis of eqns (19) and (25), the Boltzmann equilibrium solely applies at  $t \rightarrow \infty$ . Under the condition  $K_M \gg c_M^a(t)$ ,  $c_M^*(t)$  is now given in this limit by

$$c_M^*(t \rightarrow \infty) \rightarrow -(K_M / \beta_a) [k_e \tau_o / (1 + k_e \tau_L)]. \quad (29)$$

In the limits where the microorganism does not excrete metals, is uncharged and deprived of any soft surface layer ( $k_e \rightarrow 0$ ,  $y(r) \rightarrow 0$ ,  $d \rightarrow 0$ ), the expressions in Table 1, case  $\square$ , reduce to the results by Pinheiro *et al.*<sup>35</sup>

It is further possible to capture the physical meaning of the depletion timescale  $\tau_d$  by drawing an analogy with an equivalent electrochemical circuit.<sup>29,43,44</sup> After straightforward manipulations of eqns (20) and (21),  $\tau_d$  may indeed be written in the form

$$\tau_d = R_S R_e Z / (R_S + R_e), \quad (30)$$

where  $R_e \equiv R_S / (k_e \tau_L) = a^2 / (k_e G_{a,r_c})$  is a term that identifies with the resistance of the microorganism to excreting M out of its intracellular compartment, and the quantity  $Z = 4\pi (G_{a,r_c} - a^2 J_u^* \Omega_1 B n^{-1}) / S_a$  is the analogue of the Warburg impedance in electrochemistry.<sup>45</sup>  $Z$  corresponds to the extracellular mass transport impedance, while  $R_S R_e / (R_S + R_e)$  is the direct pendant of the so-called charge transfer resistance classically denoted  $R_{ct}$  in the electrochemical literature.<sup>45</sup> Within the current context,  $R_{ct}$  comprises the membrane transfer resistance  $R_S$ , *in parallel* with the resistance  $R_e$  to leakage of M from the intracellular volume.  $\tau_d$  may thus be viewed as the typical timescale for discharging the ‘capacitive’ element  $Z$  across an interface with overall metal transfer resistance  $R_S R_e / (R_S + R_e)$ .  $R_e / R_S$  may be interpreted as the ratio between the maximum uptake flux  $J_u^*$  and the excretion flux  $k_e \phi_u^*$ , with  $\phi_u^*$  the characteristic internalized metal amount defined by  $G_{a,r_c} K_M / (a^2 \beta_a)$ . As such,  $R_e / R_S$  defines a scale in the ‘vulnerability’ of the microbe to potential toxic effects following metal internalisation: the larger the ratio  $R_e / R_S$ , the longer the

residence time of M within the intracellular volume and the more likely biocompounds therein will be damaged.

Let us now examine two limiting subcases satisfying  $K_M \gg c_M^a(t)$ .

- For values of the uptake parameters  $k_{\text{int}}K_H$  and physicochemical properties of the biointerphase in line with the conditions  $Bn^{-1} = R_T/R_S \ll 1$  and  $R_T \gg 0$ , it comes  $\tau_E/\tau_L \approx 1$  and expressions of  $c_M^a(t)$  and  $c_M^*(t)$  in Table 1 (case  $\square$ ) reduce to (Supporting Information)

$$c_M^*(t) = \left( c_M^*(0) + K_M \beta_a^{-1} \frac{k_e \tau_o}{1 + k_e \tau_L} \right) e^{-t/\tau_d} - K_M \beta_a^{-1} \frac{k_e \tau_o}{1 + k_e \tau_L} = \beta_a^{-1} c_M^a(t), \quad (31)$$

where  $\tau_d \approx \tau_L / (1 + k_e \tau_L)$ . The second equality in eqn (31) marks the applicability of the Boltzmann equilibrium for M at  $t \geq 0$  as a result of fast M transport compared to actual uptake.

- In the absence of efflux ( $k_e \rightarrow 0$ ), the expression of  $c_M^*(t)$  becomes

$$c_M^*(t) = c_M^a(0) \beta_a^{-1} (1 + Bn^{-1}) e^{-t/\tau_E}. \quad (32)$$

Combination of eqns (1), (8) and (9) for  $K_M \gg c_M^a(t)$  and  $k_e \rightarrow 0$  further provides

$$c_M^a(0) = c_M^*(0) \beta_a (1 + Bn^{-1})^{-1}. \quad (33)$$

Substitution of eqn (33) into eqn (32) finally leads to

$$c_M^*(t) = c_M^*(0) e^{-t/\tau_E}, \quad (34)$$

which correctly compares with our previous result obtained for  $A = K_M / (\beta_a c_M^*) \gg 1$  in the absence of excretion.<sup>29</sup> It is straightforward to realize that condition  $K_M \gg c_M^a$  is automatically satisfied when  $A \gg 1$  because the metal surface concentration is necessarily lower or equal to the value given by Boltzmann's law ( $c_M^a \leq \beta_a c_M^*$ ).

#### 4.3. Expressions for the uptake, transport and excretion fluxes.

The equations in Table 1 cover the entire spectrum of dynamic situations in terms of kinetic limitation of the uptake rate by metal mass transport and integrate the interplay between internalisation and excretion. The quantity  $c_M^*(t)$  is accessible by experiments together with the uptake and excretion fluxes, or the time integral thereof.<sup>31</sup> Tables 2 and 3 show the expressions of  $J_u(t)$ ,  $J_e(t)$  (and  $J_M(t)$ ) and their integrals over  $t$  under conditions where none or one of the limits  $K_M \ll c_M^a(t)$  and  $K_M \gg c_M^a(t)$  are satisfied.

Results originate from the application of eqns (1), (4), (8) and (11) with substitution therein of the relevant expressions for  $c_M^*(t)$  and  $c_M^a(t)$ . Note that the internalised metal amount  $\phi_u(t)$  is equivalently evaluated from the ratio  $J_e(t)/k_e$  and from eqn (11). In addition, the systematic applicability of Boltzmann law at  $t \rightarrow \infty$  in the cases [A], [B] and [C] of Table 1 leads to  $J_M(t \rightarrow \infty) \rightarrow 0$ , which is in agreement with the results given in Table 2.

### Expressions for $J_u(t)$ , $J_e(t)$ and $J_M(t)$

$\forall K_M$ :

$$J_u(t) = J_u^* \frac{\bar{c}_M^a(t)}{1 + \bar{c}_M^a(t)} \quad J_e(t) = k_e e^{-k_e t} \left\{ \phi_u^0 + J_u^* \int_0^t \frac{\bar{c}_M^a(\xi)}{1 + \bar{c}_M^a(\xi)} e^{k_e \xi} d\xi \right\} \quad J_M(t) = R_T^{-1} \left[ c_M^*(t) - \beta_a^{-1} c_M^a(t) \right] \quad \text{[A]}$$

$K_M \ll c_M^a(t)$ :

$$J_u(t) = J_u^* \quad J_e(t) = J_u^* \left[ 1 + \left( \frac{k_e \phi_u^0}{J_u^*} - 1 \right) e^{-k_e t} \right] \quad J_M(t) = J_u^* \left\{ 1 - \left[ 1 + \left( \frac{k_e \phi_u^0}{J_u^*} - 1 \right) e^{-k_e t} \right] \right\} \quad \text{[B]}$$

$K_M \gg c_M^a(t)$ :

$$J_u(t) = J_u^* \left[ \left( \bar{c}_M^a(0) + \frac{k_e \tau_o}{1 + k_e \tau_L} \right) e^{-t/\tau_d} - \frac{k_e \tau_o}{1 + k_e \tau_L} \right]$$

$$J_e(t) = k_e e^{-k_e t} \left\{ \phi_u^0 + J_u^* \tau_o \left[ \frac{1}{1 + k_e \tau_L} - \frac{\tau_E / \tau_o}{1 + k_e (\tau_L - \tau_E)} \left( \bar{c}_M^a(0) + \frac{k_e \tau_o}{1 + k_e \tau_L} \right) \left( e^{(k_e - \tau_d^{-1})t} - 1 \right) \right] \right\} - \frac{J_u^* k_e \tau_o}{1 + k_e \tau_L}$$

$$J_M(t) = -k_e \phi_u^0 e^{-k_e t} + J_u^* \left\{ \left( \bar{c}_M^a(0) + \frac{k_e \tau_o}{1 + k_e \tau_L} \right) e^{-t/\tau_d} - k_e e^{-k_e t} \tau_o \times \left[ \frac{1}{1 + k_e \tau_L} - \frac{\tau_E / \tau_o}{1 + k_e (\tau_L - \tau_E)} \left( \bar{c}_M^a(0) + \frac{k_e \tau_o}{1 + k_e \tau_L} \right) \left( e^{(k_e - \tau_d^{-1})t} - 1 \right) \right] \right\} \quad \text{[C]}$$

**Table 2.** Expressions for the uptake, excretion and conductive diffusion fluxes.

#### 4.4. Illustrations.

Figure 2 shows the typical evolution of  $c_M^*$  with time for various metal affinity  $K_M$  values and efflux kinetic constant  $k_e$ . The physicochemical parameters adopted for the biointerphase are detailed in the caption. In particular, results are shown for the case where electrostatics is screened ( $\beta_a = f_{el} = 1$ ),  $\phi_u^0 = 0$  and the water content in the soft surface layer is so high that  $\varepsilon = D_{M,in} / D_{M,out} = 1$ . The accuracy of the

analytical expressions given in Table 1 for reproducing the exact numerical results is verified provided that conditions validating their use are satisfied. The existence of a non-zero plateau value for  $c_M^*(t \rightarrow \infty)$  is further confirmed for situations where  $k_e \neq 0$ . In the extreme where excretion is infinitely fast compared to uptake (*i.e.*  $k_e \tau_L \gg 1$  or, equivalently,  $R_S \gg R_e$ ), the efflux efficiently buffers  $c_M^*$  so that no bulk metal depletion is observed. In addition, Figures 2A and 2D show that the time constants  $1/k_e$  and  $\tau_d$  correctly identify with the key timescales for bulk metal depletion kinetics in the cases of strong and weak metal affinities, respectively. Finally, the inadequacy of eqn (28) for  $k_e \rightarrow 0$  is illustrated in Figure 2A.

### Expressions for the cumulative uptake and excretion fluxes

$\forall K_M$ :

$$\mathbf{A} \quad \int_0^t J_u(t) dt = J_u^* \int_0^t \frac{\bar{c}_M^a(\xi)}{1 + \bar{c}_M^a(\xi)} d\xi \quad \int_0^t J_e(\xi) d\xi = \phi_u^0 (1 - e^{-k_e t}) + k_e J_u^* \int_0^t e^{-k_e u} \int_0^u \frac{\bar{c}_M^a(\xi)}{1 + \bar{c}_M^a(\xi)} e^{k_e \xi} d\xi du$$

$K_M \ll c_M^a(t)$ :

$$\mathbf{B} \quad \int_0^t J_u(\xi) d\xi = J_u^* t \quad \int_0^t J_e(\xi) d\xi = J_u^* \left[ t + \frac{1}{k_e} \left( \frac{k_e \phi_u^0}{J_u^*} - 1 \right) (1 - e^{-k_e t}) \right]$$

$K_M \gg c_M^a(t)$ :

$$\mathbf{C} \quad \int_0^t J_u(\xi) d\xi = J_u^* \left\{ \frac{\tau_E}{1 + k_e \tau_L} \left[ \bar{c}_M^a(0) + \frac{k_e \tau_O}{1 + k_e \tau_L} \right] (1 - e^{-t/\tau_d}) - \frac{k_e \tau_O}{1 + k_e \tau_L} t \right\}$$

$$\int_0^t J_e(\xi) d\xi = \phi_u^0 (1 - e^{-k_e t}) + J_u^* \left\{ \frac{\tau_E}{1 + k_e \tau_L} \left[ \bar{c}_M^a(0) + \frac{k_e \tau_O}{1 + k_e \tau_L} \right] \times \right.$$

$$\left. \left( 1 - \frac{k_e \tau_E}{k_e (\tau_E - \tau_L) - 1} e^{-t/\tau_d} + \frac{1 + k_e \tau_L}{k_e (\tau_E - \tau_L) - 1} e^{-k_e t} \right) - \frac{k_e \tau_O}{1 + k_e \tau_L} \left[ t + \frac{1}{k_e} (e^{-k_e t} - 1) \right] \right\}$$

**Table 3.** Expressions for the cumulative uptake and excretion fluxes.

In Figure 3, the dependence of  $c_M^a$  on  $t$  is shown under the conditions of Figure 2. As demonstrated in §4, the equilibrium relationship  $c_M^* = \beta_a^{-1} c_M^a$  systematically applies at  $t \rightarrow \infty$  and its domain of validity extends to any  $t$  for cases where  $K_M \ll c_M^a(t)$  (Figure 3A). For situations where  $K_M \ll c_M^a(t)$  is not respected (Figures 3B-3D), the limitation of uptake by metal transport and the subsequent inapplicability of

equilibrium Boltzmann law is manifested by the deviation of the ratio  $c_M^a(0)/c_M^*(0)$  from unity. It is worthwhile to note that for cases where  $c_M^a(0)/c_M^*(0) \neq 1$ ,  $c_M^a$  may increase or decrease with  $t$  depending on  $K_M$  and  $k_e$ , which is confirmed by the evaluation of  $dc_M^a(t)/dt|_{t \rightarrow 0}$  from the expression given in Table 1, case  $\square$ . It is found that the sign for  $dc_M^a(t)/dt|_{t \rightarrow 0}$  is indeed determined by the sign of the quantity  $-(c_M^a(0)/K_M + k_e\tau_0/(1+k_e\tau_L))$  with  $-\tau_0 \geq 0$ . For the sake of completeness, the dependences of  $J_u$ ,  $J_e$  and  $J_M$  on  $t$  are shown in Supporting Information (Figure S1) for the set of parameters adopted in Figures 2-3. In agreement with theory,  $J_M(t \rightarrow \infty) \rightarrow 0$  and  $J_u(t \rightarrow \infty) = J_e(t \rightarrow \infty)$ . It was further verified that exact numerical results are correctly reproduced by the analytical expressions collected in Table 2 under the conditions  $K_M \ll c_M^a(t)$  and  $K_M \gg c_M^a(t)$ .

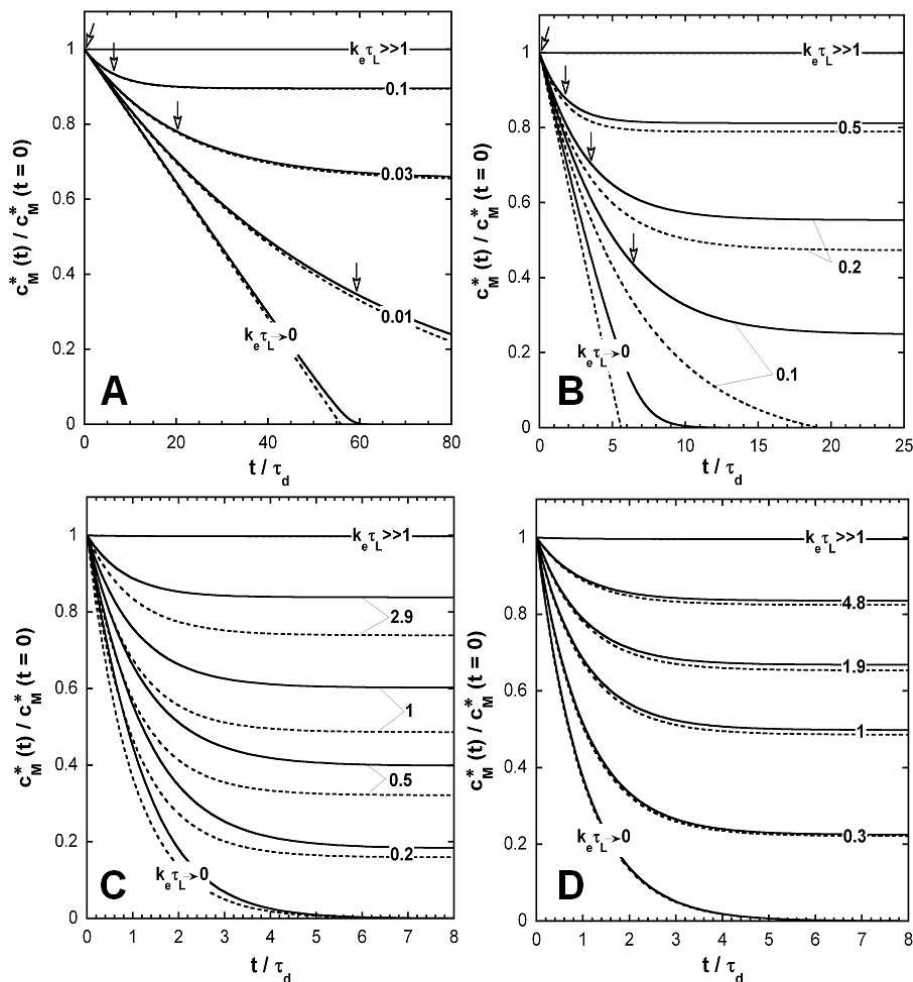


**Figure 2.** Typical dependence of the ratio  $c_M^*(t)/c_M^*(t=0)$  on the dimensionless time  $t/\tau_d$  for various values of the excretion rate constant  $k_e$ , indicated in the dimensionless form  $k_e\tau_L$ . (A)  $K_M = 10^{-7}$  mM, (B)  $K_M = 10^{-6}$  mM, (C)  $K_M = 10^{-5}$  mM and (D)  $K_M = 10^{-4}$  mM. Model parameters:  $a = 400$  nm,  $d = 50$  nm,  $\varphi = 10^{-6}$ ,  $k_{\text{int}}K_H = 2 \times 10^{-3}$  ms $^{-1}$ ,  $D_{M,\text{out}} = 10^{-9}$  m $^2$ s $^{-1}$ ,  $\varepsilon = D_{M,\text{in}}/D_{M,\text{out}} = 1$ ,  $\phi_u^0 = 0$ ,  $c_M^*(t=0) = 10^{-5}$  mM,  $z = 1$ ,  $z_M = 2$ ,  $\Gamma_{\text{max}}^s = \rho_{\text{max}}^V = 0$  (metal adsorption on the biomembrane and in the soft surface layer is ignored in eqn (18)),  $y(r) = 0$  (no electrostatics). For this set of parameters,  $\tau_L = 94.9$  s and  $\tau_E = 169.8$  s. In panels (A) and (B), the arrows correspond to the value of  $c_M^*(t)/c_M^*(t=0)$  at  $t = 1/k_e$ . The dotted lines in (A)-(B) and (C)-(D) correspond to evaluations from expressions given in Table 1, cases **B** and **C**, respectively. The adopted biouptake parameters conform to orders of magnitude given in the literature.<sup>6,11</sup>

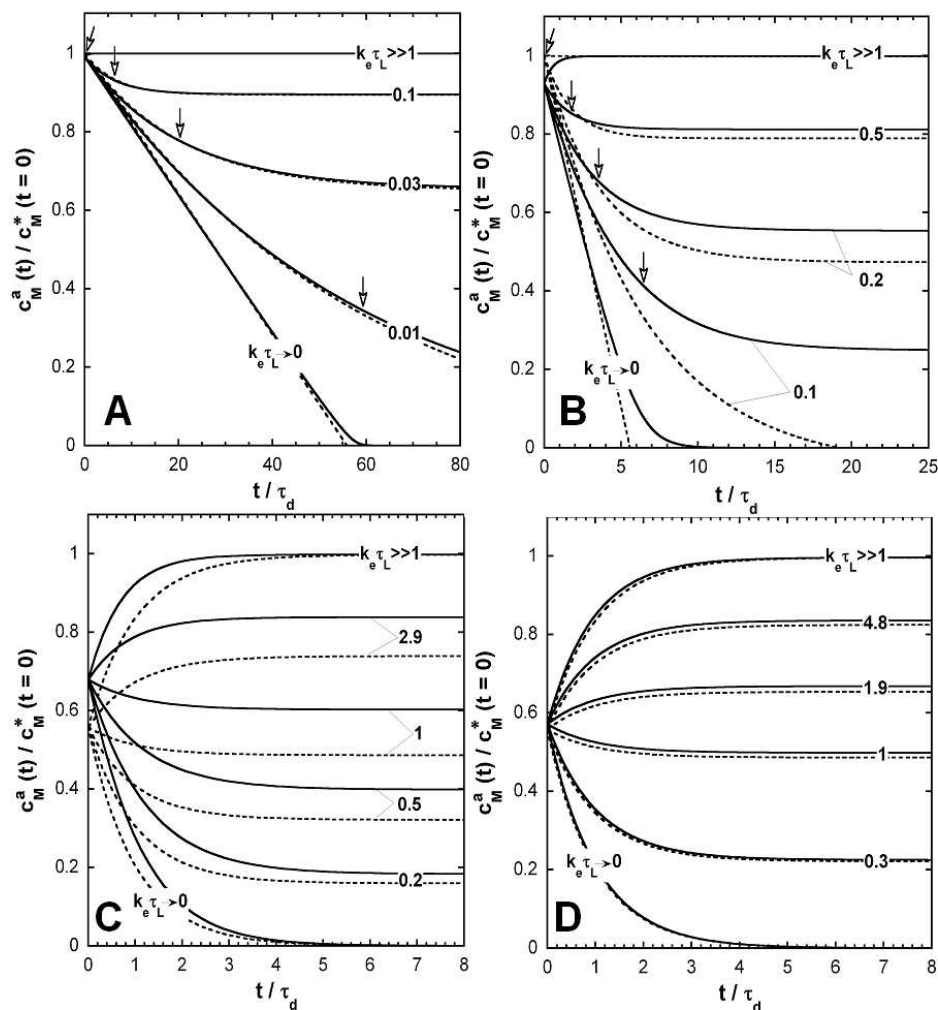


**Figure 3.** Typical dependence of the ratio  $c_M^a(t)/c_M^*(t=0)$  on the dimensionless time  $t/\tau_d$  for various values of the excretion rate constant  $k_e$ , indicated in the dimensionless form  $k_e\tau_L$ . Model parameters: as in Figure 2.

We now examine the impact of the charge carried by the microbial soft surface layer on the dynamics of metal uptake. Because electrostatics do not modulate the timescale  $1/k_e$  for depletion kinetics in the situation  $K_M \ll c_M^a(t)$ , Figure 4A shows the depletion timescale  $\tau_d = \tau_E/(1+k_e\tau_L)$  (relevant in the limit  $K_M \gg c_M^a(t)$ ) for various values of  $k_e$  and the dimensionless ratio  $-\rho_0/(2Fzc^\infty)$ , where  $\rho_0$  is the density of negative charges supported by the soft surface layer ( $\rho_0 \leq 0$ ).<sup>29</sup> The quantity  $\rho_0/(2Fzc^\infty)$  determines the sign and magnitude of the electrostatic interaction potential  $y(r)$  between microbe and metals, as discussed elsewhere.<sup>19,29</sup> In the absence of excretion,  $\tau_d (= \tau_E)$  decreases with increasing

$-\rho_0/(2Fzc^\infty)$  because depletion kinetics becomes more rapid when favouring attractive interactions between microbes and M, which conforms with the predictions from a previous study.<sup>29</sup> For a fixed  $-\rho_0/(2Fzc^\infty)$ ,  $\tau_d$  decreases with increasing  $k_e$ , which is in agreement with the equation  $\tau_d = \tau_E/(1+k_e\tau_L)$ : the faster the excretion process, the faster the plateau value  $c_M^*(\infty)$  is reached over time (Figure 2). Figure 4A further shows that  $\tau_d$  becomes nearly independent of  $k_e$  for  $-\rho_0/(2Fzc^\infty) \gg 1$  and under such extreme electrostatic conditions, the membrane transfer resistance  $R_s = 1/(k_{\text{int}}K_H b_a)$  tends to zero following a dramatic increase in  $b_a$ , so that  $\tau_L \rightarrow 0$  and  $\tau_d \rightarrow \tau_E$ . In turn, this explains why the interplay between metal excretion kinetics and electrostatics may result in fast or sluggish bulk metal depletion depending on  $k_e$  and  $-\rho_0/(2Fzc^\infty)$ .

In Figure 4B, the dependence of  $c_M^*(\infty)$  and  $J_u(\infty)$  on  $k_e$  and  $-\rho_0/(2Fzc^\infty)$  are given under the conditions adopted in Figure 4A. Unsurprisingly,  $c_M^*(\infty)$  increases for increasing values of  $k_e$  under fixed electrostatic conditions (Figure 2). In addition,  $c_M^*(\infty)$  decreases with increasing  $-\rho_0/(2Fzc^\infty)$  at a fixed  $k_e$  as a result of enhanced metal depletion following the increase in the attractive interaction potential between microbe and M. Note that for a sufficiently large  $-\rho_0/(2Fzc^\infty)$ ,  $c_M^*(\infty)$  reaches a value that is nearly independent of  $-\rho_0/(2Fzc^\infty)$ . This feature can not be simply demonstrated analytically and it likely results from the weak dependence of  $\tau_L$  on electrostatics for  $-\rho_0/(2Fzc^\infty) \gg 1$ .<sup>29</sup> Figure 4B shows the expected increase in  $J_u(\infty)(=J_e(\infty))$  with  $k_e$  and further indicates the ratio  $J_u(\infty)/J_u^*$  increases with increasing attractive interaction between M and microorganism. Since metal transport does not limit the uptake at  $t \rightarrow \infty$  where the equilibrium Boltzmann law applies, this increase in uptake flux is explained by the decrease in membrane transfer resistance  $R_s$ . The pendant of Figures 4A&B for situations where the microbial soft surface layer is positively charged (due to e.g. the sorption of abiotic materials onto the membrane) is given in Supporting Information (Figure S2).

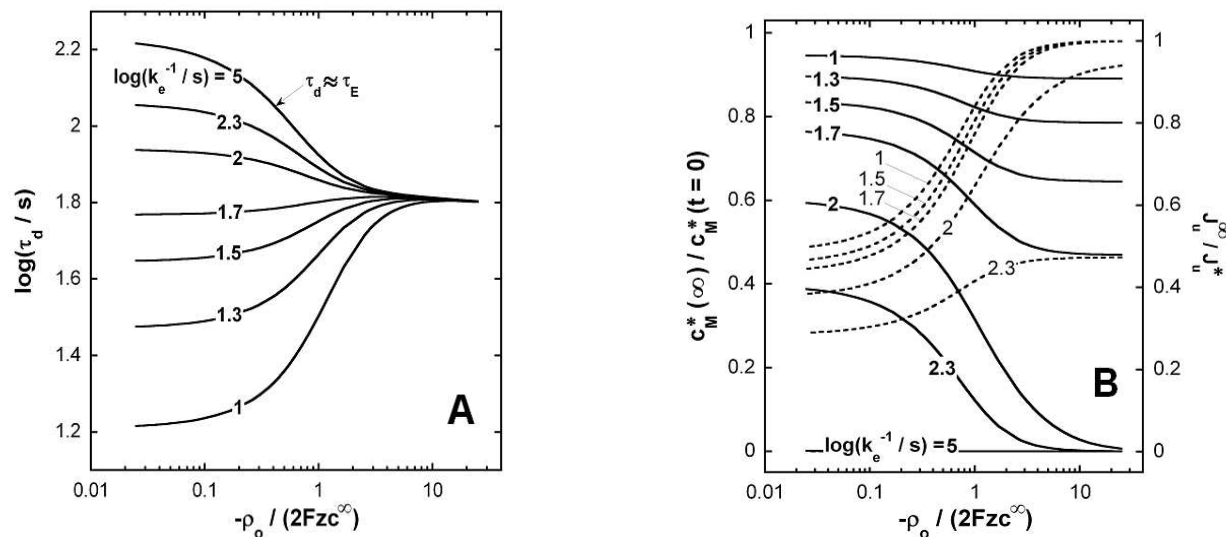


**Figure 4.** (A) Dependence of the characteristic depletion timescale  $\tau_d$  on the dimensionless charge  $-\rho_o / (2Fzc^\infty)$  of the soft surface layer for various values of  $1/k_e$  (indicated). Model parameters :  $K_M = 10^{-5}$  mM, and  $\rho_o / F = -50$  mM.<sup>6,11,17</sup> Other parameters:  $a = 400$  nm,  $d = 50$  nm,  $\varphi = 10^{-6}$ ,  $k_{\text{int}}K_H = 2 \times 10^{-3}$  ms<sup>-1</sup>,  $D_{M,\text{out}} = 10^{-9}$  m<sup>2</sup>s<sup>-1</sup>,  $\varepsilon = 1$ ,  $\phi_u^0 = 0$ ,  $c_M^*(t=0) = 10^{-5}$  mM,  $z = 1$ ,  $z_M = 2$ ,  $\Gamma_{\text{max}}^S = \rho_{\text{max}}^V = 0$  (metal adsorption on the biomembrane and in the soft surface layer is ignored in eqn (18)), and  $\mathfrak{T} = \varepsilon_s / \varepsilon_r = 1$ ,  $y_a = \bar{\sigma}_a = 0$ <sup>29</sup> (the membrane surface is uncharged). (B) Dependence of the ratios  $c_M^*(t \rightarrow \infty) / c_M^*(t=0)$  (plain lines) and  $J_u^\infty / J_u^*$  (dotted lines) under the conditions of panel (A).

For the sake of completeness, Figure 5 reports the typical variations in  $c_M^*$  and  $c_M^a$  with  $t$  for various values of  $\rho_o / (2Fzc^\infty)$  that cover cases where the soft surface layer is negatively and positively charged and the results obtained from the expressions given in Table 2 are also provided for comparison purpose. In line with expectations, depletion is gradually favoured (suppressed) upon increase of the attractive (repulsive) interaction potential between M and the microbe, which is accompanied by an enhancement (reduction) of the metal surface concentration  $c_M^a$ . Electrostatics thus largely modulate the amount of bioavailable metals, *i.e.* metals that are located at the membrane surface where internalisation sites are distributed.

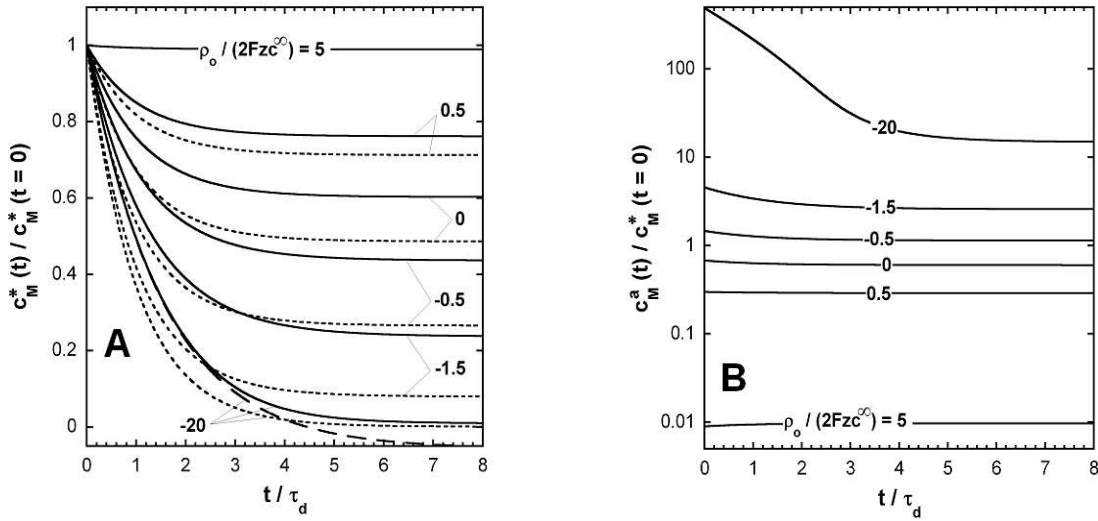


**Figure 5.** Typical dependence of (A)  $c_M^*(t)/c_M^*(t=0)$  and (B)  $c_M^a(t)/c_M^*(t=0)$  on  $t/\tau_d$  for various values of  $\rho_o/(2zFc^\infty)$ . Model parameters:  $\log(k_e^{-1}/s) = 2$  and  $c^\infty = 10$  mM. Other model parameters: as in Figure 4. The short dotted lines in (A) correspond to evaluation from expressions in Table 1, case [C] and the long dotted line to computations from expressions in Table 1, case [B].

## 5. Situations where 2D and 3D metal adsorptions are relevant.

### 5.1. General formulation.

In the most complex scenario where adsorption of M on the biomembrane surface and across the 3D soft shell layer must be included in the mass balance equation,<sup>31</sup> elimination of  $c_M^*(t)$  using eqn (13) leads, after lengthy algebra, to the intricate differential equation in  $c_M^a(t)$  given in Supporting Information (eqn (S41) therein). This equation may be simplified for cases where the adsorption on the membrane surface is much more significant than that across the soft surface layer, *i.e.*  $Q^V(t) \rightarrow 0$  in eqn (18), which in turn leads to

$$\left\{ \frac{(\tau_L - \tau_E) - \tau_L \left[ 1 + \bar{c}_M^a(t) \right]^2 - \tau_S \left[ \frac{1 + \bar{c}_M^a(t)}{1 + \theta \bar{c}_M^a(t)} \right]^2}{\left[ 1 + \bar{c}_M^a(t) \right] \left\{ \bar{c}_M^a(t) + k_e \left[ 1 + \bar{c}_M^a(t) \right] \left[ \tau_o + \bar{c}_M^a(t) \left[ \tau_L + \frac{\tau_S}{1 + \theta \bar{c}_M^a(t)} \right] \right] \right\}} \right\} d\bar{c}_M^a(t) = dt, \quad (35)$$

where  $\theta = K_M/K_M^S$  and  $\tau_S = \theta \Gamma_{\max}^S / J_u^* = k_{\text{int}}^{-1} K_H^S / K_H$  is the characteristic timescale for internalizing metal amount  $\theta \Gamma_{\max}^S$  under conditions where efflux is insignificant and uptake flux equates  $J_u^*$ . For the

limit  $\tau_S \rightarrow 0$ , eqn (35) correctly reduces to eqn (19). Evaluation of  $c_M^a(t)$  and  $c_M^*(t)$  from eqn (15), (35) or eqn (S41) requires numerical computation performed here according to COLSYS<sup>42</sup> collocation algorithm. Like the situation treated in §4, the problem may be solved rigorously under the limits of strong and weak metal affinities.

5.1.1. Limit of strong metal affinities :  $K_M, K_M^S \ll c_M^a(t)$  and  $K_M^V \ll c_M(r,t)$ .

Provided that all these inequalities apply, eqns (1)-(3) simplify to  $J_u(t) \approx J_u^*$ ,  $\Gamma^S(t) \approx \Gamma_{\max}^S$  and  $Q^V(t) = V_{\text{soft}} \rho_{\max}^V$ , respectively, where  $V_{\text{soft}}$  is the volume of the soft surface layer. After substitution within eqns (15) and (18) and solving of the resulting differential equation, the expressions of  $c_M^a(t)$  and  $c_M^*(t)$  are identical to those given in Table 1, case [B], replacing  $\tau_0$  by the timescale  $\tilde{\tau}_0$  defined by (Supporting Information)

$$\tilde{\tau}_0 = \tau_0 + \left( \Gamma_{\max}^S + V_{\text{soft}} \rho_{\max}^V / S_a \right) / J_u^* \quad (36)$$

where  $\tau_0$  is given by eqn (26). As in §4.1, the equilibrium distribution of M in the extracellular volume applies here at  $t \geq 0$  while the equations for fluxes and cumulative fluxes given in Tables 2 and 3 (case [B]) also remain correct pending the replacement of  $\tau_0$  by  $\tilde{\tau}_0$ . The quantity  $J_u^*(\tilde{\tau}_0 - \tau_0)$  in eqn (36) simply corresponds to the total amount of metal ions ‘neutralized’ by the microbe *via* 2D and 3D adsorption on sites located on the membrane and within the soft surface structure.

5.1.2. Limit of weak metal affinities :  $K_M, K_M^S \gg c_M^a(t)$  and  $K_M^V \gg c_M(r,t)$

In this situation, the isotherms describing the adsorption of M on the internalisation sites and the mere adsorption sites may be linearized. After combination of eqns (15) and (18), we show that the searched  $c_M^a(t)$  and  $c_M^*(t)$  are defined by the expressions reported in Table 1, case [C], where the timescales  $\tau_L$  and  $\tau_E$  are now replaced by  $\tilde{\tau}_L$  and  $\tilde{\tau}_E$ , respectively, with  $\tilde{\tau}_L$  and  $\tilde{\tau}_E$  defined by (Supporting Information)

$$\tilde{\tau}_L = -K_M \beta_a^{-1} \left( 2\Omega_2 x_a + \Omega_1 x^* \right) + \tau_S \quad (37)$$

and

$$\tilde{\tau}_E = \tilde{\tau}_L - J_u^* \Omega_1 R_T x^* + \tau_S \quad (38)$$

The time constant  $\tau_S$  corrects  $\tau_{L,E}$  for adsorption of M on the membrane surface while the dimensionless scalar  $x_a (\geq 1)$  and  $x^* (\geq 1)$  in eqns (37)-(38) correct  $\tau_{L,E}$  for adsorption of M across the soft surface layer according to (Supporting Information):

$$x_a = 1 - \rho_{\max}^V \left( 2\Omega_2 a^2 K_M^V J_u^* \right)^{-1} \left( G_{a,r_0} + H_{a,r_0}^a a \varepsilon^{-1} f_{el} \right), \quad (39)$$

and

$$x^* = 1 + H_{a,r_0}^a a \varepsilon^{-1} f_{el} \rho_{\max}^V \left( \Omega_1 a^2 K_M^V J_u^* \right)^{-1}, \quad (40)$$

where  $\Omega_1$ ,  $\Omega_2$ ,  $G_{r_1,r_2}$  and  $H_{r_1,r_2}^r$  were defined in §4. The fluxes and cumulative fluxes corresponding to the case of interest here, may be evaluated from the expressions provided in Tables 2 and 3, case  $\square$ , substituting  $\tilde{\tau}_L$  and  $\tilde{\tau}_E$  for  $\tau_L$  and  $\tau_E$ , respectively. Following the interpretation done in §4.2 in terms of an equivalent electrochemical circuit (eqn (30)), the timescale  $\tilde{\tau}_d = \tilde{\tau}_E / (1 + k_e \tilde{\tau}_L)$  now involved in  $c_M^a(t)$  and  $c_M^*(t)$  may be formulated as  $\tilde{\tau}_d = \tilde{R}_S R_e \tilde{Z} / (\tilde{R}_S + R_e)$ , where the membrane transfer resistance  $\tilde{R}_S$  and metal transport impedance  $\tilde{Z}$  are now defined by

$$\tilde{R}_S / R_S = 1 + \tau_S / \tau_L - K_M \beta_a^{-1} \left[ 2\Omega_2 (x_a - 1) + \Omega_1 (x^* - 1) \right] / \tau_L \quad (41)$$

and

$$\tilde{Z} = 4\pi \left( G_{a,r_c} - a^2 J_u^* \Omega_1 \tilde{B} n^{-1} \right) / S_a, \quad (42)$$

with  $\tilde{B} n^{-1} = \tilde{R}_T / \tilde{R}_S$  and  $\tilde{R}_T = x^* R_T$ . Stated differently, 2D and 3D adsorption of metals *effectively* lead to an increase in the membrane transfer and mass transport resistances  $R_S$  and  $R_T$ , respectively, since  $x_a \geq 1$ ,  $x^* \geq 1$ ,  $\Omega_1 \leq 0$  and  $\Omega_2 \leq 0$  (Supporting Information, §SI2 and §SI6). This is an elegant way to quantify the role played by metal adsorbing compounds of the biointerphase in protecting the sensitive intracellular compartment against potentially toxic metals. In the limit where the adsorption of M on sites across the microbial surface layer is insignificant,  $\rho_{\max}^V \rightarrow 0$  and/or  $K_M^V \rightarrow \infty$ ,  $x_a = x^* = 1$  and  $\tilde{\tau}_{L,E}$  reduce to  $\tau_{L,E} + \tau_S$ . As a remark, the ‘Model of Uptake with Instantaneous Adsorption and Efflux’ (MUIAE) derived by Hadju et al.<sup>31</sup> corresponds to the specific limit  $x_a = x^* = 1$ ,  $\beta_a = f_{el} = 1$  and  $R_T = 0$  because the authors considered *a priori* that the rate of uptake is limited by internalisation only and that electrostatics can be neglected (despite the low 5 mM electrolyte concentration used in their experiments). Under such restrictive conditions,  $\tilde{\tau}_d$  becomes  $\tilde{\tau}_d = (\tau_L + \tau_S) / [1 + k_e (\tau_L + \tau_S)]$ . Using the expression of  $\tau_L$  derived elsewhere,<sup>29</sup> we obtain after arrangements

$$\tilde{\tau}_d = \left( V_c S_a^{-1} + K_H^S \right) / \left[ k_{int} K_H + k_e \left( V_c S_a^{-1} + K_H^S \right) \right], \quad (43)$$

where  $V_c$  is the volume of the Kuwabara unit cell. Equation (43) correctly merges with the result given by Hadju et al.<sup>31</sup>

## 5.2. Illustration and comments.

Figure 6 shows typical time-dependent profiles for  $c_M^*$  under conditions where metal ions adsorb on mere adsorption sites located at the membrane surface only, and the soft surface layer surrounding the microorganism membrane is either uncharged (Figures 6A&B) or carries a charge  $\rho_0$  (Figures 6C&D). Results are reported for various values of the affinity parameter  $K_M^S$ .

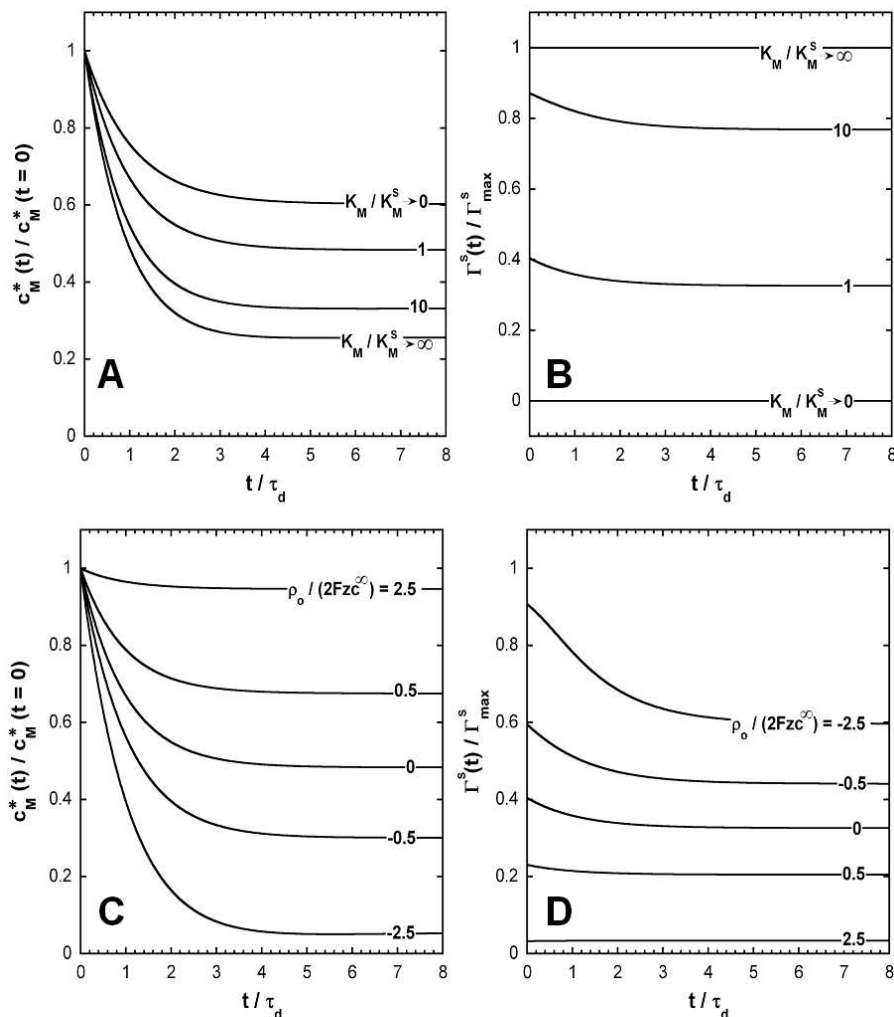


**Figure 6.** (A) Typical dependence of  $c_M^*(t)/c_M^*(t=0)$  on the dimensionless time  $t/\tau_d$  for various values of the ratio  $K_M/K_M^S$  and (B) corresponding time-dependence of the surface coverage  $\Gamma^S/\Gamma_{\max}^S$  due to adsorption of M on the membrane. Model parameters:  $a = 400$  nm,  $d = 50$  nm,  $\varphi = 10^{-6}$ ,  $K_M = 10^{-5}$  mM,  $k_{\text{int}}K_H = 2 \times 10^{-3}$  ms $^{-1}$ ,  $D_{M,\text{out}} = 10^{-9}$  m $^2$ s $^{-1}$ ,  $\varepsilon = 1$ ,  $\phi_u^0 = 0$ ,  $c_M^*(t=0) = 10^{-5}$  mM,  $z = 1$ ,  $z_M = 2$ ,  $\rho_{\max}^V = 0$ ,  $\Gamma_{\max}^S = 10^{-6}$  mol m $^{-2}$ ,  $\log(k_e^{-1}/s) = 2$  and  $y(r) = 0$  (no electrostatics). Panels (C) and (D): parameters identical to (A) and (B), respectively, except that the dimensionless charge  $\rho_0/(2zFc^\infty)$  of the soft layer is varied and  $K_M = K_M^S = 10^{-5}$  mM,  $c^\infty = 10$  mM and the membrane surface is uncharged. Biouptake and adsorption parameters

conform to orders of magnitude given in the literature.<sup>6,11,31</sup>

We systematically verified that the analytical expressions derived in §5.1.1 and §5.1.2 correctly reproduce the numerical results within the time domain where the conditions justifying their use are satisfied (data not shown). As intuitively expected, the magnitude of  $c_M^*(t)$  decreases at a fixed  $t$  with increasing the affinity of M for the adsorption sites on the membrane surface, *i.e.* for decreasing values of  $K_M^S$  (Figure 6B). These trends are enhanced by increasing the negative charge carried by the soft surface layer (Figures 6C&D), *i.e.* with increasing the magnitude of the (negative) electrostatic potential across the soft biointerphase.

On a qualitative level, the profiles  $c_M^*(t)$  computed for various affinities, electrostatic and excretion parameters exhibit similar patterns (Figures 2, 5, 6). However, the theory quantitatively demonstrates how the timescales, the exponential prefactors and  $c_M^*(\infty)$  values involved in the expression of  $c_M^*(t)$  are determined by the internalisation, excretion, adsorption and metal transport features which are modulated by changing operational parameters such as electrolyte concentration and solution pH (that both affect  $y(r)$  and thus  $\tau_{L,E}$ ) or microorganism volume fraction  $\phi$ . Therefore, a complete and univocal interpretation of metal uptake dynamics at complex soft charged biointerphases necessarily requires the measurement of depletion profiles under various physico-chemical medium compositions. The benefit in varying  $\phi$  will be detailed in a forthcoming publication where the current theory will be successfully tested by experiments using model bacterial strains with different aptitudes to excrete metal ions. Alternative approaches include the systematic measurements over time of the adsorbed, internalized and bulk metal concentrations, a time demanding strategy that is rarely found in literature.<sup>31</sup> However, extensive analysis of such data does not exclude the necessity to account for electrostatics, to verify the relevance of the adopted linear Henry adsorption regime, or quantify the validity of the often postulated equilibrium distribution of M in the extracellular volume. The flexibility of the theory detailed here allows for addressing these issues. Other studies are based on the *ad hoc* adjustment of metal adsorption isotherms on microorganisms according to Langmuir or Freundlich type of expressions.<sup>32-34</sup> This work clearly demonstrates that such approaches are not sufficient to decipher the biophysicochemical processes controlling metal internalisation (and subsequent toxicity) or microbial resistance to metals.

## 6. Conclusions.

A generic formalism is developed for metal uptake dynamics at complex microbial interphases. The model integrates the basic physicochemical descriptors of the active biointerphase with the size and volume fraction of the microorganism, the interfacial distribution of electrostatic charges, the permittivity of the peripheral surface appendage(s) and its ability to impede metal diffusion toward the membrane. The theory

accounts for the impacts over time of metal depletion, internalisation, excretion and adsorption of metals at the biomembrane or across the soft surface layer it supports. The exact differential equations governing biouptake kinetics are derived and compared with analytical and tractable expressions developed for situations where the affinities of metal ions for internalisation and mere adsorption sites are weak or strong. The corresponding equations defining the time dependence of the experimentally-accessible uptake and excretion fluxes are further provided. The theory allows for estimating the key timescale for bulk metal depletion kinetics as a function of the biophysicochemical properties of the microbial interphase, electrolyte concentration, pH or the microorganism volume fraction. A rigorous expression is further derived for the non-zero plateau value reached by bulk metal concentration at sufficiently long times as a result of metal excretion. Finally, physical quantities are given in the form of resistive circuit elements to address the respective contributions of metal excretion, transport, adsorption and internalisation in defining metal bioaccumulation and resistance of microbes to potential toxic effects. Remaining challenges include the extension of the current theory to aquatic media containing metal-complexing (nano)particles or mixtures of metal ions, other microorganism geometries and to situations where microorganismal growth and death kinetics interfere with metal uptake dynamics. The theory offers a robust physicochemical basis to formulate these practical cases.

**Supporting Information.** (i) Detailed derivations of eqns (16), (19), (31), (36)-(40), expressions given in Table 1 and of the differential equations governing  $c_M^a(t)$  with account of 2D and 3D adsorptions. A rigorous demonstration of the inequality  $\Omega_1 \leq 0$ , which corrects a mistake in Ref. [29]. The inequalities  $-\tau_o \geq 0$ ,  $x_a \geq 1$ ,  $x^* \geq 1$  and  $\Omega_2 \leq 0$  are derived and the equality  $\alpha_1 = 0$  is shown to hold when  $\phi_u^0 = 0$ . (ii) Plots of  $J_u(t)$ ,  $J_e(t)$  and  $J_M(t)$  for the set of parameters adopted in Figures 2-3 (Figure S1). (iii) Pendant of Figures 4A&B for cases where the microbial soft surface layer is positively charged (Figure S2).

**Acknowledgements.** J.F.L.D. acknowledges the European Commission's seventh framework program (project BIOMONAR: theme 2: Food, Agriculture and Biotechnology, grant agreement 244405) for financial support.

#### List of main symbols.

- $a$  Radius of the intracellular component of the microorganism.
- $A$  Dimensionless metal-membrane surface affinity parameter.
- $B$  Bioconversion capacity of the microorganism.
- $Bn = A/B$  Bioavailability number.
- $c_M^*$  Bulk metal concentration.
- $c_M^a$  Metal concentration at the membrane surface.
- $\bar{c}_M^a$  Dimensionless metal concentration at the membrane surface ( $\bar{c}_M^a = c_M^a / K_M$ ).
- $\bar{c}_\pm$  Constants defined by eqn (23).  $\bar{c}_+$  corresponds to  $\bar{c}_M^a(t \rightarrow \infty)$ .

- $c^\infty$  Bulk concentration of ions from background electrolyte.  
 $c_p$  Microorganism number concentration.  
 $d$  Thickness of the soft surface layer.  
 $D_{M,in}$ ,  $D_{M,out}$  Metal diffusion coefficient inside and outside the microbial soft surface layer.  
 $f_{el}$  Conductive diffusion factor pertaining to the whole biointerphase.  
 $f_{el,in}$  Conductive diffusion factor pertaining to the soft surface layer.  
 $f_{el,out}$  Conductive diffusion factor pertaining to the medium outside the soft surface layer.  
 $F_{r_1,r_2}$  Integral function defined by  $\int_{r_1}^{r_2} r^{-2} b_r^{-1} dr$  ( $m^{-1}$ ).  
 $G_{r_1,r_2}$  Integral function defined by  $\int_{r_1}^{r_2} r^2 \beta_r dr$  ( $m^3$ ).  
 $H_{r_1,r_2}^{r_3}$  Integral function defined by  $\int_{r_1}^{r_2} r^2 \beta_r F_{r,r_3} dr$  ( $m^2$ ).  
 $J_e$  Metal excretion flux.  
 $J_u$  Metal internalisation flux.  
 $J_M$  Incoming flux of metals at the membrane surface.  
 $J_M^*$  Limiting incoming flux of metals at the membrane surface.  
 $J_u^*$  Limiting metal internalisation flux.  
 $K_H$  Henry coefficient pertaining to the internalisation sites (m).  
 $K_H^S$  Henry coefficient pertaining to the mere adsorption sites on the membrane surface (m).  
 $K_M$  Metal-internalisation site affinity parameter ( $mol\ m^{-3}$ ).  
 $K_M^S$  Affinity of M for the mere adsorption sites on the membrane surface ( $mol\ m^{-3}$ ).  
 $K_M^V$  Affinity of M for the mere adsorption sites across the soft surface layer ( $mol\ m^{-3}$ ).  
 $k_e$  Kinetic constant for metal excretion ( $s^{-1}$ ).  
 $k_{int}$  Kinetic constant for metal internalisation ( $s^{-1}$ ).  
 $M^{z_M}$  Metal ions of valence  $z_M$ .  
 $r$  Radial coordinate system.  
 $r_c$  Radius of the Kuwabara cell.  
 $r_0 = a + d$  Radius of the microorganism including the peripheral soft surface layer.  
 $Q^V$  Amount of metals adsorbed in the soft surface layer.  
 $R_e$  Microorganism resistance to excrete metal ions ( $m^{-1}s$ ).  
 $R_s$  Membrane transfer resistance ( $m^{-1}s$ ).  
 $R_T$  Conductive diffusional metal transfer resistance ( $m^{-1}s$ ).  
 $R_s^0$  Membrane transfer resistance corrected for adsorption of M ( $m^{-1}s$ ).  
 $R_T^0$  Conductive diffusional metal transfer resistance corrected for adsorption of M ( $m^{-1}s$ ).  
 $S_a$  Surface area of the nude microorganism (without the soft surface layer).  
 $t$  Time.

$y(r)$  Dimensionless electrostatic potential at the position  $r$ .

$z$  Valence of background electrolyte ions.

$z_M$  Valence of metal ions.

$Z$  Mass transport impedance equivalent of the Warburg element in electrochemistry.

$\tilde{Z}$  Mass transport impedance corrected for adsorption of M.

#### Greek symbols

$b_a$  Boltzmann surface term.

$b_r$  Function of  $r$  defined by  $\exp(-z_M y(r)/z)$ .

$e$  Defined by the ratio  $D_{M,in}/D_{M,out}$ .

$e_r$  Relative dielectric permittivity of the medium.

$e_s$  Relative dielectric permittivity of the microbial soft surface layer.

$\phi$  Volume fraction of microorganisms.

$\phi_u$  Concentration of internalized metals per microorganism surface area ( $\phi_u(t=0) = \phi_u^0$ ).

$\Gamma^S$  Surface concentration of metals adsorbed on the membrane.

$\Gamma_{\max}^S$  Surface concentration of adsorption sites at the membrane.

$\hat{A}$  Ratio defined by  $e_s/e_r$ .

$\Omega_{1,2}$  Coefficients that depend on the potential distribution and  $e$  ( $\text{mol}^{-1}\text{m}^3\text{s}$ ).

$r_o$  Volume density of charges distributed throughout the soft surface layer.

$r_{\max}^V$  Volume density of adsorption sites in the soft surface layer.

$\tau_E, \tilde{\tau}_E$  Time constants defined by eqns (21), (38) respectively.

$\tau_L, \tilde{\tau}_L$  Time constants defined by eqns (20), (37) respectively.

$\tau_d, \tilde{\tau}_d$  Characteristic depletion timescales for M depletion kinetics with and without account of adsorption.

$\tau_S$  Time constant defined by  $\tau_S = \theta \Gamma_{\max}^S / J_u^* = k_{\text{int}}^{-1} K_H^S / K_H$ .

$\tau_o, \tilde{\tau}_o$  Time constants defined by eqns (24) and (36), respectively.

$\theta$  Ratio  $K_M / K_M^S$ .

$\omega^0$  Ratio  $\omega^0 = k_e \phi_u^0 / J_u^*$ .

$\tilde{\nu}$  Ratio  $\varepsilon_s / \varepsilon_r$ .

#### References.

1. I. Worms, D. F. Simon, C. S. Hassler and K. J. Wilkinson, *Biochimie*, 2006, **88**, 1721-1731.
2. J. Galceran and H. P. van Leeuwen, in *Physicochemical kinetics and transport at biointerfaces*, eds H. P. van Leeuwen and W. Köster, John Wiley, Chichester, 2004, Chapter 4, pp. 147.
3. H. P. van Leeuwen, R. M. Town, J. Buffle, R. F. M. J. Cleven, W. Davison, J. Puy, W. H. van Riemsdijk and Laura Sigg, *Environ. Sci. Technol.*, 2005, **39**, 8545-8556.
4. H. P. van Leeuwen, *Environ. Sci. Technol.*, 1999, **33**, 3743-3748.
5. J. P. Pinheiro and H. P. van Leeuwen, *Environ. Sci. Technol.*, 2001, **35**, 894-900.
6. V. I. Slaveykova and K. J. Wilkinson, *Environ. Chem.*, 2005, **2**, 9-24.

7. K. J. Wilkinson and J. Buffle, in *Physicochemical kinetics and transport at biointerfaces*, eds H. P. van Leeuwen and W. Köster, John Wiley & Sons, Chichester, 2004, Chapter 10, pp. 445.
8. P. Sánchez-Marín, C. Fortin, and P. G. C. Campbell, *Environ. Chem.*, 2013, **10**, 80-90.
9. C. Fortin and P. G. C. Campbell, *Environ. Toxicol. Chem.*, 2000, **19**, 2769-2778.
10. A. Crémazy, P. G. C. Campbell and C. Fortin, *Environ. Sci. Technol.*, 2013, **47**, 2408-2415.
11. C. S. Hassler and K. J. Wilkinson, *Environ. Toxicol. Chem.*, 2003, **22**, 620-626.
12. T. N. P. Bosma, P. J. M. Middeldorp, G. Schraa and A. J. B. Zehnder, *Environ. Sci. Technol.*, 1997, **31**, 248-252.
13. J. F. L. Duval, H. J. Busscher, B. van de Belt-Gritter, H. C. van der Mei, and W. Norde, *Langmuir*, 2005, **21**, 11268-11282.
14. F. Gaboriaud, M. L. Gee, R. Strugnell and J. F. L. Duval, *Langmuir*, 2008, **24**, 10988-10995.
15. G. Francius, P. Polyakov, J. Merlin, Y. Abe, J.-M. Ghigo, C. Merlin, C. Beloin and J. F. L. Duval, *PLoS ONE*, 2011, **6(5)**, e20066.
16. R. Mikutta, A. Baumgärtner, A. Schippers, L. Haumaier and G. Guggenberger, *Environ. Sci. Technol.*, 2012, **46**, 3866-3873.
17. J. F. L. Duval and F. Gaboriaud, *Curr. Opin. Colloid Interface Sci.*, 2010, **15**, 184-195.
18. A. Clements, F. Gaboriaud, J. F. L. Duval, J. L. Farn, A. W. Jenney, T. Lithgow, O. L. C. Wijburg, E. L. Hartland and R. A. Strugnell, *PLoS ONE*, 2008, **3**, e3817.
19. J. Merlin and J. F. L. Duval, *Phys. Chem. Chem. Phys.*, 2012, **14**, 4491-4504.
20. C. Pagnout, S. Jomini, M. Dadhwal, C. Caillet, F. Thomas, P. Bauda, *Colloids Surf. B Biointerfaces*, 2012, **92**, 315-321.
21. M.-E. Krapf, B. S. Lartiges, C. Merlin, G. Francius, J. Ghanbaja and J. F. L. Duval, *Water Research*, 2012, **46**, 1838-1846.
22. M. W. Pabst, C. D. Miller, C. O. Dimkpa, A. J. Anderson, and J. E. McLean, *Chemosphere*, 2010, **81**, 904-910.
23. A. G. González, L. S. Shirokova, O. S. Pokrovsky, E. E. Emnova, R. E. Martínez, J. M. Santana-Casiano, M. González-Dávila, and G. S. Pokrovski, *J. Colloid Interface Sci.*, 2010, **350**, 305-314.
24. J. Ha, A. Gelabert, A. M. Spormann, and G. E. Brown, *Geochim. Cosmochim. Acta*, 2010, **74**, 1-15.
25. O. Zeyons, A. Thill, F. Chauvat, N. Menguy, C. Cassier-Chauvat, C. Oréar, J. Daraspe, M. Auffan, J. Rose, O. Spalla, *Nanotoxicology*, 2009, **3**, 284-295.
26. J. Liu, J. Ma, C. He, X. Li, W. Zhang, F. Xu, Y. Lin and L. Wang, *New Phytologist*, 2013, **200**, 691-699.
27. E. Wasserman, A. R. Felmy, and A. Chilakapati, *Colloids Surf. B Biointerfaces*, 2000, **18**, 19-29.
28. C. Liu, J. M. Zachara, A. Felmy, and Y. Gorby, *Colloids Surf. B Biointerfaces*, 2004, **38**, 55-65.

29. J. F. L. Duval, *Phys. Chem. Chem. Phys.*, 2013, **15**, 7873-7888.
30. J. B. Best, *Cell Comp. Physiol.*, 1955, **46**, 1-27.
31. R. Hajdu, J. P. Pinheiro, J. Galceran, and V. I. Slaveykova, *Environ. Sci. Technol.*, 2010, **44**, 4597-602
32. G. Vijayakumar, R. Tamilarasan and M. Dharmendra Kumar, *Chemical Engineering Research Bulletin*, 2011, **15**, 18-24.
33. A. Öztürk, T. Artan and A. Ayar, *Colloids Surf. B Biointerfaces*, 2004, **34**, 105-111.
34. M. M. Areco and M. dos Santos Afonso, *Colloids Surf. B Biointerfaces*, 2010, **81**, 620-628.
35. J. P. Pinheiro, J. Galceran and H. P. van Leeuwen, *Environ. Sci. Technol.*, 2004, **38**, 2397-2405.
36. M. L. Sorongon, R. A. Bloodgood and R. P. Burchard, *Appl. Environ. Microbiol.*, 1991, **57**, 3193-3199.
37. C. Xu, S. Zhang, C.-Y. Chuang, E. J. Miller, K. A. Schwehr and P. H. Santschi, *Marine Chem.* 2011, **126**, 27-36.
38. H. P. van Leeuwen, J. Buffle and R. Town, *Langmuir* 2012, **28**, 227-234.
39. H. P. van Leeuwen and J. Buffle, *Environ. Sci. Technol.* 2009, **43**, 7175-7183.
40. J. F. L. Duval and H. P. van Leeuwen, *J. Phys. Chem. A* 2012, **116**, 6443-6451.
41. J. Galceran and H. P. van Leeuwen, in *Physicochemical kinetics and transport at biointerfaces*, eds H. P. van Leeuwen and W. Köster, John Wiley, Chichester, 2004, Chapter 4, pp. 152.
42. U. Ascher, J. Christiansen and R. D. Russel, *ACM Trans. Math. Software*, 1981, **7**, 209-222.
43. R. J. M. Hudson, *Sci. Total. Environ.*, 1998, **219**, 95-115.
44. K. B. Oldham, J. C. Myland, in *Steady-state voltammetry. Fundamentals of electrochemical science*, Academic press, San Diego, 1994, pp. 263-308.
45. A. J. Bard and L. R. Faulkner, in *Electrochemical methods*, John Wiley & Sons, New York, 2nd edn, 2001, p. 376.